

Journal of Building Engineering

Porosity-based models for estimating the mechanical properties of self-compacting concrete with coarse and fine recycled concrete aggregate

--Manuscript Draft--

Manuscript Number:	
Article Type:	Research Paper
Section/Category:	Building materials
Keywords:	recycled concrete aggregate; self-compacting concrete; mechanical behavior; effective capillary porosity; non-linear multiple regression
Corresponding Author:	Víctor Revilla-Cuesta University of Burgos: Universidad de Burgos Burgos, SPAIN
First Author:	Víctor Revilla-Cuesta
Order of Authors:	Víctor Revilla-Cuesta Flora Faleschini Mariano A. Zanini Marta Skaf Vanessa Ortega-López
Abstract:	<p>The mechanical properties of concrete containing Recycled Concrete Aggregate (RCA) and their prediction generally depend on the RCA fraction in use. In this study, porosity indices are applied to develop predictive equations for the estimation of the mechanical properties of Self-Compacting Concrete (SCC), regardless of the RCA fraction and amount in use. A total of ten SCC mixes were prepared, nine of which containing different proportions of coarse and/or fine RCA (0%, 50% or 100% for both fractions), and the tenth mixed with 100% coarse and fine RCA and also RCA powder 0-1 mm. The following properties were evaluated: compressive strength, modulus of elasticity, splitting tensile strength, flexural strength, and effective porosity as measured with the capillary-water-absorption test. Negative effects on the above properties were recorded for increasing contents of both RCA fractions. The application of simple regression models yielded porosity-based estimations of the mechanical properties of the SCC with an accuracy margin of $\pm 20\%$, regardless of the RCA fraction and amount. The multiple regression models, developed with the compressive strength as a second prediction variable, presented even tighter accuracy margins at $\pm 10\%$ and showed greater robustness, so that any variation in porosity had little significant effect on prediction accuracy. Furthermore, porosity predictions using the 24-h effective water also yielded accurate estimations of all the above mechanical properties. Finally, comparisons with the results of other studies validated the reliability of the models and their accuracy, especially the minimum expected values at a 95% confidence level, at all times lower than the experimental results.</p>
Suggested Reviewers:	<p>Miren Etxeberria, PhD Professor, Universitat Politècnica de Catalunya: Universitat Politècnica de Catalunya miren.etxeberria@upc.edu Expert in characterization and use of recycled concrete aggregates in building and civil engineering applications. She has been author of several articles about the behavior of concrete manufactured with recycled concrete aggregate in the last ten years.</p> <p>José Matos, PhD Professor, University of Minho: Universidade do Minho jmatos@civil.uminho.pt Expert on the topics of structural engineering as well as on the reuse of waste in cement based materials for building and civil applications.</p> <p>Asad-ur-Rehman Khan, PhD Professor, University of Karachi asadkhan@neduet.edu.pk</p>

	Expert in characterization and use of construction and demolition waste in building and civil engineering applications. He has been author of articles with this item for the last ten years.
Opposed Reviewers:	



Víctor Revilla-Cuesta
Department of Civil Engineering
University of Burgos
EPS. Calle Villadiego, s/n
09001 BURGOS
SPAIN

Journal of Building Engineering

Editors-in-Chief: J. de Brito, J. M. LaFave, R. Yao

September, 2021

Dear Sirs,

Herewith, please find appended the article entitled “Porosity-based models for estimating the mechanical properties of self-compacting concrete with coarse and fine recycled concrete aggregate”, by Víctor Revilla-Cuesta, Flora Faleschini, Mariano A. Zanini, Marta Skaf and Vanesa Ortega-López for publication in the Journal of Building Engineering.

Existing procedures for estimating the mechanical properties of concrete made with Recycled Concrete Aggregate (RCA) are generally conditioned by the added fraction of this waste. This paper aims to show that the use of porosity, either measured experimentally or estimated indirectly through the effective water of the concrete mix, allows accurate estimation of these properties without the need to explicitly differentiate the fraction of RCA added.

This study applies this idea to Self-Compacting Concrete. For this purpose, 10 SCC mixes with coarse and/or fine RCA were prepared and their mechanical properties (compressive strength, modulus of elasticity, splitting tensile strength, and flexural strength) and effective porosity were determined. Simple-regression models that allowed accurate estimation of the mechanical properties regardless of the RCA fraction used were developed. However, the development of multiple-regression models with the compressive strength as a second predictor variable provided greater accuracy and robustness to this estimation. The validation of these models using results from other studies in the literature shows the usefulness and reliability of the models obtained.

Finally, I confirm this paper is our original unpublished work and it has not been submitted to any other journal for reviews.

We hope you will consider our article in a favorable light for publication in the Journal of Building Engineering.

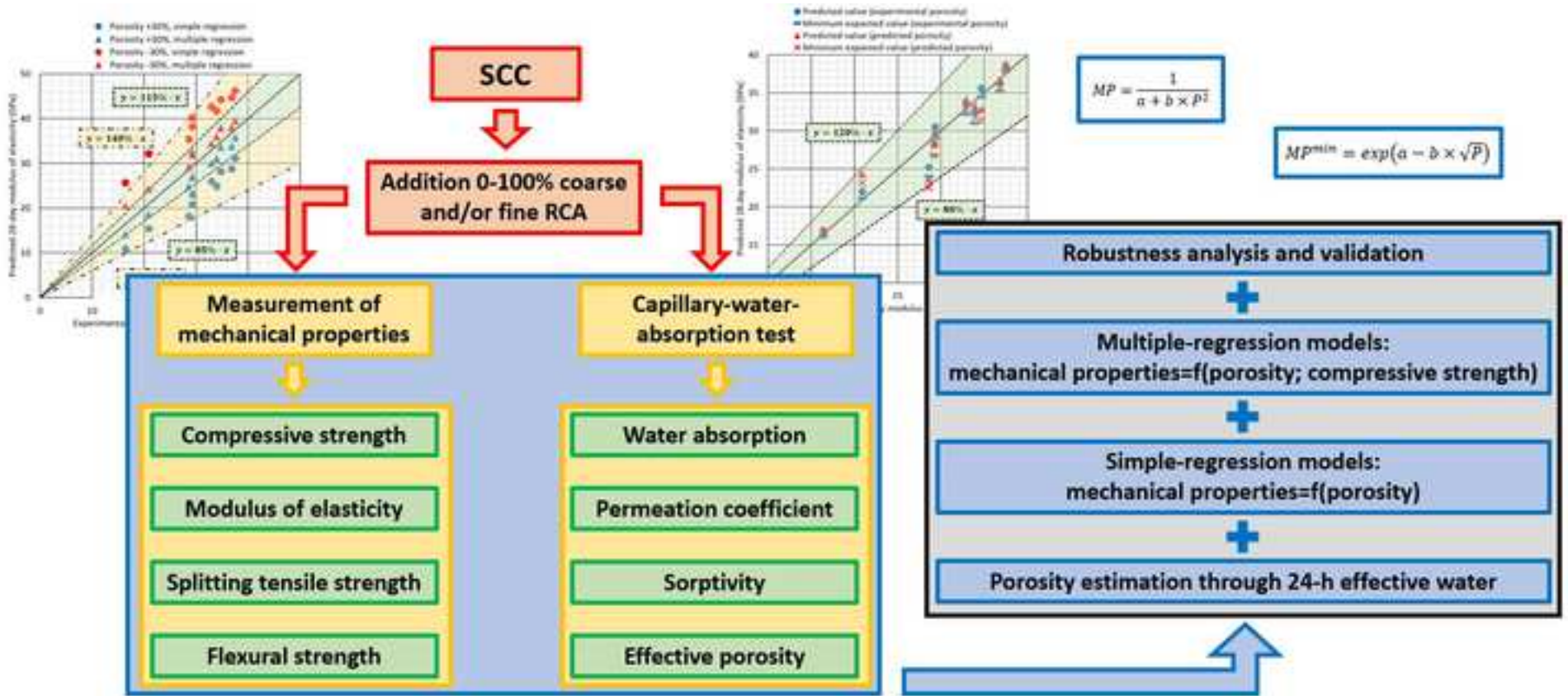
With many thanks.

Yours sincerely,

A handwritten signature in black ink, appearing to read 'V. Revilla-Cuesta'.

Víctor Revilla-Cuesta

- Mechanical behavior and porosity of SCC with coarse and/or fine RCA measured
- In general, no interaction between RCA fractions regarding mechanical properties
- 24-h effective water and RCA fractions interaction conditioned porosity estimation
- Simple-regression models precisely estimated mechanical properties through porosity
- Higher precision and robustness by compressive-strength multiple-regression models



1 Porosity-based models for estimating the mechanical properties of self- 2 compacting concrete with coarse and fine recycled concrete aggregate

3 Víctor Revilla-Cuesta ^{a,*}, Flora Faleschini ^b, Mariano A. Zanini ^b, Marta Skaf ^c, Vanesa Ortega-López ^{a,b}

4 ^a Department of Civil Engineering, Escuela Politécnica Superior, University of Burgos, c/ Villadiego s/n, 09001
5 Burgos, Spain.

6 Emails: vrevilla@ubu.es; vortega@ubu.es

7 ^b Department of Civil, Environmental and Architectural Engineering (ICEA), University of Padova, via
8 Francesco Marzolo 9, 35131 Padova, Italy.

9 Email: flora.faleschini@dicea.unipd.it; marianoangelo.zanini@dicea.unipd.it; vortega@ubu.es

10 ^c Department of Construction, Escuela Politécnica Superior, University of Burgos, c/ Villadiego s/n, 09001
11 Burgos, Spain.

12 Emails: mskaf@ubu.es

13 ***Corresponding Author:**

14 Víctor Revilla-Cuesta

15 Department of Civil Engineering, University of Burgos.

16 Escuela Politécnica Superior. Calle Villadiego s/n, 09001 Burgos, Spain.

17 Phone: +34947497117

18 e-mail: vrevilla@ubu.es

19 **Abstract**

20 The mechanical properties of concrete containing Recycled Concrete Aggregate (RCA) and their prediction
21 generally depend on the RCA fraction in use. In this study, porosity indices are applied to develop predictive
22 equations for the estimation of the mechanical properties of Self-Compacting Concrete (SCC), regardless of
23 the RCA fraction and amount in use. A total of ten SCC mixes were prepared, nine of which containing
24 different proportions of coarse and/or fine RCA (0%, 50% or 100% for both fractions), and the tenth mixed
25 with 100% coarse and fine RCA and also RCA powder 0-1 mm. The following properties were evaluated:
26 compressive strength, modulus of elasticity, splitting tensile strength, flexural strength, and effective porosity
27 as measured with the capillary-water-absorption test. Negative effects on the above properties were
28 recorded for increasing contents of both RCA fractions. The application of simple regression models yielded
29 porosity-based estimations of the mechanical properties of the SCC with an accuracy margin of $\pm 20\%$,
30 regardless of the RCA fraction and amount. The multiple regression models, developed with the compressive
31 strength as a second prediction variable, presented even tighter accuracy margins at $\pm 10\%$ and showed
32 greater robustness, so that any variation in porosity had little significant effect on prediction accuracy.
33 Furthermore, porosity predictions using the 24-h effective water also yielded accurate estimations of all the
34 above mechanical properties. Finally, comparisons with the results of other studies validated the reliability
35 of the models and their accuracy, especially the minimum expected values at a 95% confidence level, at all
36 times lower than the experimental results.

37 **Keywords:** recycled concrete aggregate; self-compacting concrete; mechanical behavior; effective capillary
38 porosity; non-linear multiple regression.

39 **Acronyms:** ANalysis Of VAriance (ANOVA); Interfacial Transition Zone (ITZ); Natural Aggregate (NA); Recycled
40 Concrete Aggregate (RCA); Self-Compacting Concrete (SCC); Water-to-Cement (w/c).

41 1. Introduction

42 Concrete is made by mixing cement, water, aggregate and, on occasions, admixtures. Any air that is not
43 released as concrete sets is occluded within the concrete matrix [1]. Moreover, the delayed reaction between
44 water and cement, as well as the water evaporation during the setting process, results in the appearance of
45 small pockets of air within the concrete mass, which were previously saturated with water [2]. Both aspects
46 explain why concrete is a porous material, despite its robustness in the hardened state [3].

47 Over recent years, various methods have been developed for accurate evaluation of concrete porosity. On
48 the one hand, computerized axial tomography scanning (CT scan) of specimens can determine pore sizes of
49 up to 100-200 μm in diameter [4]. However, continuous improvement of CT scan technology has resulted in
50 micro computed tomography (μCT scan) of increasingly higher resolution and power that now enable the
51 detection of smaller pore sizes and, therefore, more accurate estimations of concrete porosity [5]. On the
52 other hand, mercury intrusion porosimetry testing can also be used to evaluate concrete porosity, through
53 an analysis of mercury penetration within the concrete under increasing pressure [6]. The sensitivity of
54 mercury intrusion porosimetry is greater than μCT scan, in so far as pore sizes of up to 1-5 nm in diameter
55 may be detected, which in turn results in even more accurate estimations of concrete porosity [7].
56 Nevertheless, the orthodox technique for the evaluation of concrete porosity is the test of capillary water
57 absorption [8]. The slow absorption of water by concrete throughout this test and the low surface tension of
58 water mean that air can be efficiently expelled and the accessible porosity of the concrete can be accurately
59 estimated by differences in weight [1]. Furthermore, this simple low-cost test needs no special apparatus for
60 its performance [9]. The disadvantage of this test is that isolated pores that are inaccessible to water cannot
61 be evaluated, which implies slight underestimations of concrete porosity [10].

62 The development of these techniques accompanies research lines on porosity and the extent to which
63 porosity can be used as an indicator for the estimation of other concrete properties [11]. Firstly, concrete
64 porosity and its variations over time are increasingly studied and observations suggest that it fundamentally
65 evolves during the first sixteen hours, due to cement hydration, after which it remains constant [12].
66 Secondly, the influence and explanatory power of porosity on concrete durability has also been analyzed
67 [13]. Undoubtedly, external aggressive agents penetrate the concrete through the interconnected porous
68 network that is created [10]. Finally, the effects of porosity on concrete and its potential as an accurate
69 indicator of mechanical properties has been studied, so that any strength-related concrete variable may be
70 accurately estimated [14]. The results of the literature show that porosity can even explain the fatigue life of
71 concrete [15].

72 These analyses are nevertheless complex, due to the large number of factors on which the porosity of
73 concrete depends. On the one hand, the mixing process affects porosity, as fast mixing usually leads to

74 increased porosity [13]. On the other hand, the higher the Water-to-Cement (w/c) ratio, the higher porosity,
75 due to the evaporation of larger volumes of water during concrete setting [16]. Furthermore, the use of
76 admixtures usually increases concrete porosity because of the chemical reactions between them and some
77 other components of the concrete mix [17]. The modification of the cement-to-aggregate ratio also alters
78 the interactions between the components, once again varying porosity levels [10]. These aspects mean that
79 individual porosity analyses are necessary in each situation whenever the proportion of any concrete
80 component or the mixing method vary.

81 Different concrete types are developed through the above-mentioned composition modifications described
82 in the previous paragraph [18], leaving each type of concrete with its own porosity patterns [19]. For instance,
83 Self-Compacting Concrete (SCC), characterized by high filling and consistent flowability, needs no vibration
84 during placement [20]. Plasticizer admixtures and ultrafine aggregate, commonly limestone filler, as well as
85 a low coarse aggregate content, are used to reach such a high workability [21, 22]. Both aspects generally
86 imply higher porosity levels in SCC than in conventional vibrated concrete [23].

87 A current trend in the construction sector is to increase the sustainability of concrete through the use of
88 alternative aggregates and binders [24-26], which also vary the porosity level of concrete and its relationship
89 with other properties of this construction material [27]. Recycled Concrete Aggregate (RCA) consists of
90 crushed concrete elements [28]. The use of both coarse and fine fractions of RCA, in substitution of Natural
91 Aggregate (NA), tends to worsen the mechanical behavior of concrete [29, 30], due to three fundamental
92 aspects. First, the possible presence of contaminants in the fine fraction, such as gypsum [31]. In principle, if
93 RCA fines are sourced from faulty concrete components rejected in the precast industry, the presence of
94 such contaminants will be reduced [16]. Secondly, the reduced adhesion of the Interfacial Transition Zones
95 (ITZ) is notable, due to adhered mortar [30]. If coarse RCA fractions are used, then that effect is more
96 noticeable [32]. Finally, the resulting increase in porosity due to the worsening interaction and affinity of this
97 residue with cement when compared to NA [33]. Porosity increases are higher when fine RCA is used [34].

98 Attempts to analyze the effect of RCA on concrete by separately studying both coarse and fine fractions have
99 been reported in the literature [35, 36]. Furthermore, there are multiple studies that seek to estimate the
100 mechanical properties of RCA concrete, including SCC, based on properties such as compressive strength,
101 depending on the added fraction of RCA [29, 37]. However, the increased porosity levels following the
102 addition of both fractions may be used to assess and estimate the mechanical properties of concrete.
103 Accordingly, the aim of this study is to demonstrate that porosity is a magnitude that can be linked to the
104 mechanical behavior of SCC, regardless of the RCA fraction in use and the amounts of RCA that are added.
105 The main novelty of this research work is the demonstration that the mechanical behavior of recycled
106 aggregate SCC can be correlated with its porosity levels through accurate simple-regression and multiple-

107 regression mathematical models, regardless of the RCA fraction used and its amount in the SCC mix.

108 Furthermore, it will be demonstrated in this study that porosity can be estimated according to the
109 composition of the SCC.

110 Ten SCC mixes of similar flowability were prepared, incorporating 0%, 50% and 100% coarse and/or fine RCA.

111 One of the 100% mixes also included RCA powder. In all the mixtures, in addition to slump flow and viscosity,

112 the most relevant mechanical properties were measured: 7-day and 28-day compressive strength, modulus

113 of elasticity at 7 and 28 days, 28-day splitting tensile strength, and flexural strength at 28 days. Moreover,

114 the porosity of all the mixtures was determined through the capillary-water-absorption test. This test was

115 selected because it is simple and cheap to implement [9]. Finally, the relationship between all the mechanical

116 properties and porosity was analyzed in detail through accurate simple- and multiple-regression statistical

117 models for porosity-based estimations of the mechanical behavior of SCC containing RCA, regardless of the

118 fraction and the amount of added RCA.

119 **2. Materials and methods**

120 **2.1. Materials**

121 All the mixes were prepared with ordinary Portland cement (CEM I 52.5 R), as per EN 197-1 [38], with a

122 specific gravity of around 3.1 Mg/m³, and potable water. In addition, two admixtures were added: a

123 plasticizer and a setting regulator. Their purpose was to increase the flowability of the SCC and to reduce the

124 water content required for adequate self-compactability [35].

125 Both coarse (4-12 mm) and fine (0-4 mm) fractions of siliceous NA of a rounded shape were used, suitably

126 sized for an appropriate SCC mix. Their density and water absorption levels in 24 h and 15 minutes (Table 1)

127 represented common values [39]. However, as shown in Figure 1, the fine fraction showed an insufficient

128 fines content to achieve optimum self-compactability. For this reason, limestone powder 0-1 mm, a material

129 commonly used to manufacture mortars [40], was also added to SCC. Likewise, its main physical properties

130 and particle gradation are respectively shown in Table 1 and in Figure 1.

Table 1. Physical properties of aggregates

	Siliceous NA 4-12 mm	Siliceous NA 0-4 mm	Limestone powder 0-1 mm	RCA 4-12 mm	RCA 0-4 mm	RCA 0-1 mm
Saturated-surface- dry density (Mg/m ³)	2.61	2.57	2.61	2.43	2.38	2.36
24-h water absorption (% wt.)	0.84	0.25	0.53	6.25	7.36	7.47
15-min water absorption (% wt.)	0.71	0.18	0.38	4.90	5.77	6.26

132 In the sample mixes of this study, both coarse and fine RCA was used in substitution of 50% and 100% of

133 coarse and fine NA. The RCA was from crushed concrete components rejected immediately after their

134 manufacture at a minimum compressive strength of 45 MPa. For one of the mixes, the RCA was ground and

135 sieved to obtain RCA powder (0-1 mm) that replaced limestone powder. The density of this waste was lower
 136 than that of NA, while its water absorption was notably higher regardless of the time period (Table 1) [39].
 137 The RCA showed a continuous particle gradation, suitable for the production of concrete and similar to that
 138 of NA (Figure 1). The fine fraction of RCA had a higher fines content than the fine siliceous NA.

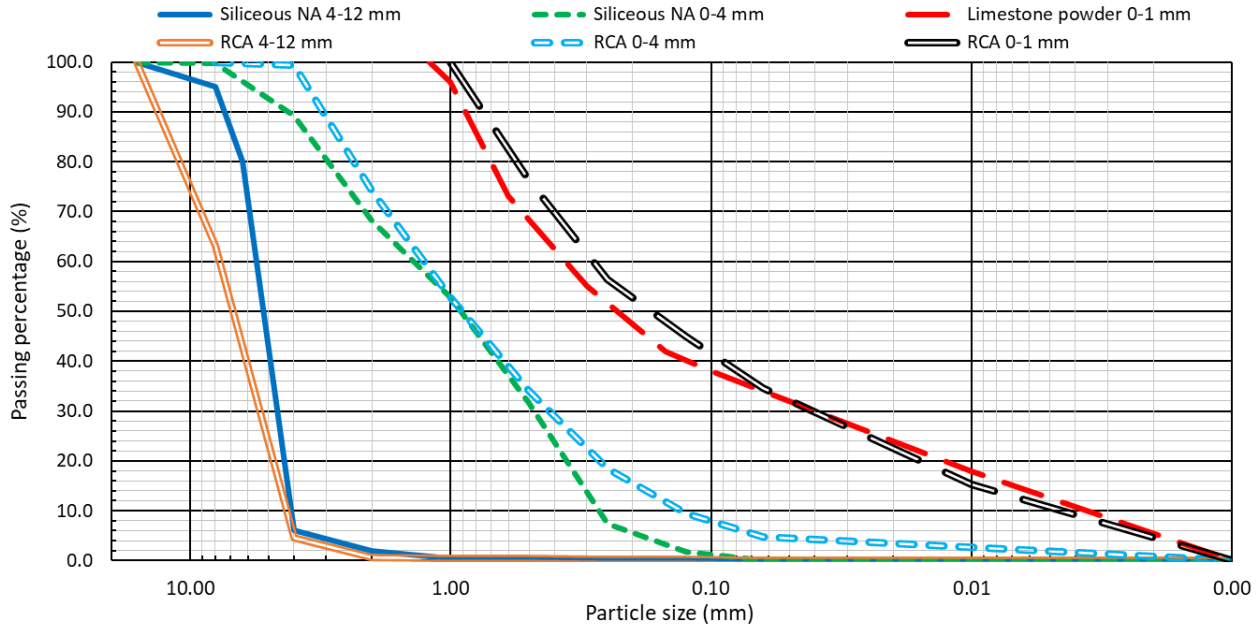


Figure 1. Particle gradation of the aggregates

2.2. Mix design

In total, 10 mixes were prepared to evaluate the performance of all possible combinations of coarse and fine RCA. The mix-design process was sequential:

- Initially, the reference mix was produced with 0% coarse and fine RCA (100% coarse and fine siliceous NA). The proportions of the different components were initially set according to Eurocode 2 indications [41], although these values were then empirically adjusted to achieve an adequate slump flow of around 750 mm.
- Afterwards, 50% or 100% coarse and/or fine siliceous NA was replaced with RCA of the same fraction by volume correction. The replacement percentages were defined in accordance with the conclusions of a previous study by the authors [32], in which three RCA contents with a similar statistical effect on the mechanical behavior of SCC were detected: 0-25%, 50% and 75-100%.
- Finally, in the mix with 100% coarse and fine RCA, limestone powder was replaced with RCA 0-1 mm. The objective was to study the behavior of a mix made with full RCA replacement of all aggregate fractions.

In all the mixtures, the water content was adjusted according to water absorption of the aggregate within 15 minutes (Table 1), *i.e.*, the duration of the mixing process. Therefore, the water content was increased when

157 RCA, which has higher water absorption levels than NA, was added [42]. In this way, a constant effective w/c
 158 ratio (value of 0.50) could be maintained and, in turn, a slump flow between 700 mm and 800 mm in all the
 159 mixes was obtained. Thus, it was ensured that water had no effect on the results and the effect of the RCA
 160 additions could be precisely studied [43].

161 The mix composition is depicted in Table 2, and, as an example, the joint particle gradation of the mixes
 162 produced with 50% coarse RCA and variable amounts of fine RCA is shown in Figure 2. The correct fit of the
 163 mixes to the Fuller curve may be noted with regard to the proportion of particles smaller than 0.25 mm, thus
 164 guaranteeing adequate self-compactability [27]. The mixtures were labelled "XCYF", where X and Y
 165 represented the percentage of coarse and fine RCA additions, respectively (0%, 50% and 100%). The letters
 166 C and F after the amounts referred to the coarse (C) and fine (F) percentile fractions of RCA. The mixture
 167 incorporating RCA powder 0-1 mm was coded with an R at the end.

Table 2. Mix composition (kg per cubic meter)

SCC mix	Cement	Water	Coarse NA # RCA	Fine NA # RCA	Limestone # RCA powder	Plasticizer	Setting regulator
0C0F	300	160	580 # 0	940 # 0	340 # 0	4.50	2.20
0C50F	300	180	580 # 0	470 # 435	340 # 0	4.50	2.20
0C100F	300	205	580 # 0	0 # 870	340 # 0	4.50	2.20
50C0F	300	170	290 # 270	940 # 0	340 # 0	4.50	2.20
50C50F	300	195	290 # 270	470 # 435	340 # 0	4.50	2.20
50C100F	300	215	290 # 270	0 # 870	340 # 0	4.50	2.20
100C0F	300	180	0 # 540	940 # 0	340 # 0	4.50	2.20
100C50F	300	205	0 # 540	470 # 435	340 # 0	4.50	2.20
100C100F	300	230	0 # 540	0 # 870	340 # 0	4.50	2.20
100C100FR	300	245	0 # 540	0 # 870	0 # 305	4.50	2.20

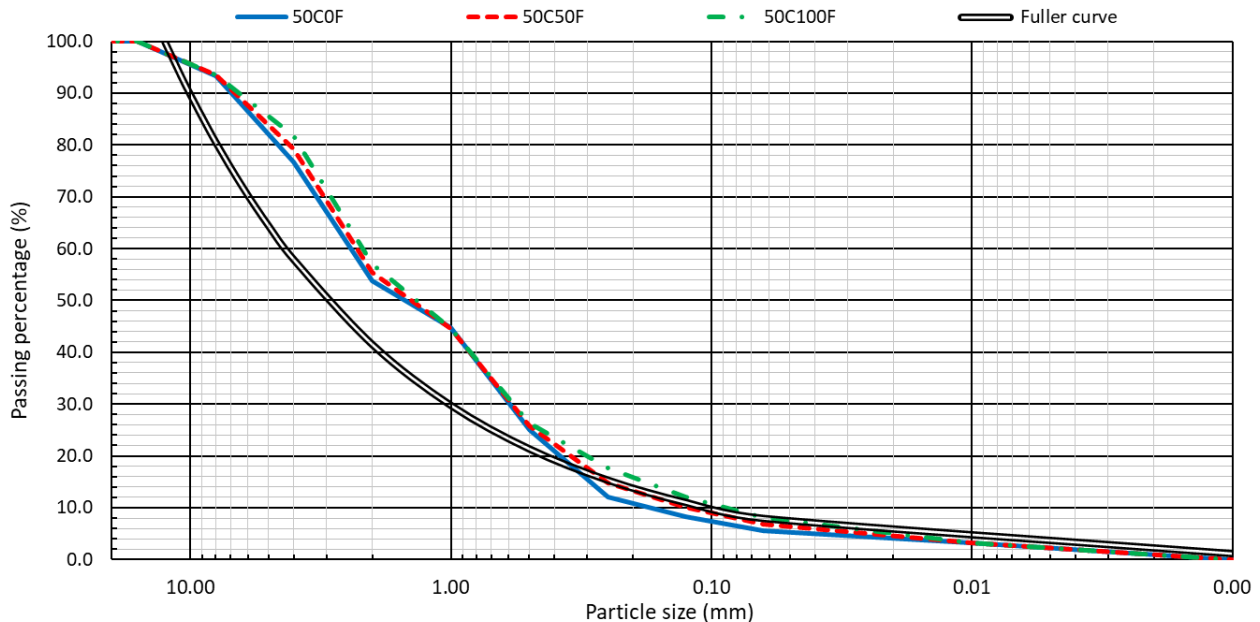


Figure 2. Joint particle gradation of the SCC mixes

171 2.3. Mixing process

172 A staged mixing process was conducted to maximize the flowability of SCC and to ensure an adequate level

173 of porosity in all mixtures [44], since rapid mixing generally increases the capillary porosity of the
 174 cementitious matrix [13]. This mixing process consisted of three stages, so that different SCC components
 175 were added at each stage, as detailed in Figure 3. After each stage, the SCC was mixed and left to rest for
 176 three and two minutes, respectively. Through several experimental trials, these mixing and resting times
 177 were found to maximize the flowability of SCC.

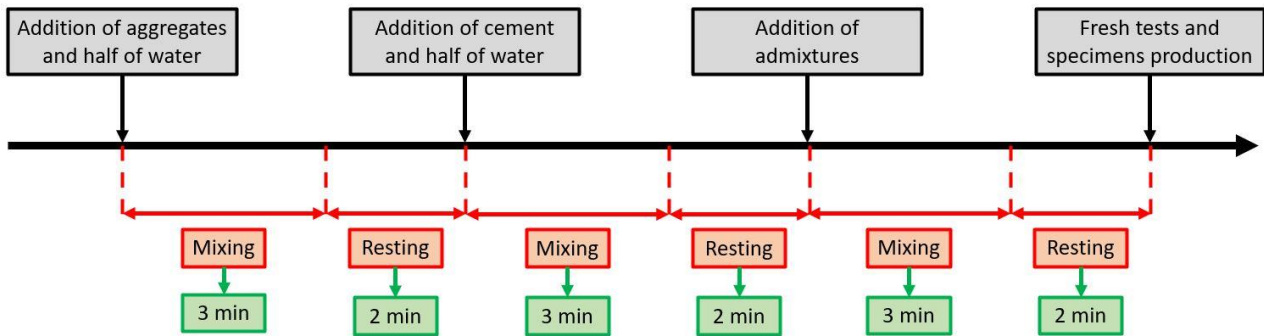


Figure 3. Mixing process

2.4. Experimental tests

181 Once the mixing process was completed, the slump-flow test (EN 12350-8 [38]) was performed, thus
 182 determining both slump flow and viscosity t_{500} . The slump flow of all the mixes had to be 750 ± 50 mm, to
 183 ensure that the mix water had no influence on the results, so that the effect of RCA could be clearly analyzed
 184 [43]. Subsequently, the specimens for all the hardened-state tests were prepared. The results of each
 185 property were determined through the values obtained in two different specimens. The specimens produced
 186 for each mix were:

- Eight 100x200-mm cylindrical specimens to measure the compressive strength (EN 12390-3 [38]) and the modulus of elasticity (12390-13 [38]) at 7 and at 28 days, as well as the 28-day splitting tensile strength (EN 12390-6 [38]).
- Two 75x75x275-mm prismatic specimens for measuring flexural strength at 28 days (EN 12390-5 [38]).
- Two 100x100x100-mm cubic specimens for the capillary-water-absorption test as per RILEM CPC 11.2 [45]. Performed at 28 days, this test was used to estimate the accessible porosity of the mixtures, which was subsequently related to their mechanical properties.

3. Results and discussion

3.1. Slump flow and viscosity

197 The slump flow and viscosity t_{500} of all the mixes were measured immediately after the mixing process. In this
 198 way, the ability of the SCC mixes to fill the formwork and the speed at which this filling would be performed

199 could be evaluated [42]. Table 3 shows the slump flow and viscosity t_{500} of the mixtures with an accuracy of
 200 ± 5 mm and ± 0.2 s, respectively. In addition, the percentage variations of both properties when adding coarse
 201 and/or fine RCA is also shown.

Table 3. Slump flow and viscosity t_{500}

SCC mix	Slump flow (mm)	Viscosity t_{500} (s)	Δ coarse RCA ¹ (%)	Δ fine RCA ² (%)	Δ coarse and fine RCA ³ (%)	Δ RCA powder ⁴ (%)
OCOF	765	2.6	-/-	-/-	-/-	-/-
OC50F	780	2.6	-/-	+2.0/0.0	+2.0/0.0	-/-
OC100F	810	3.0	-/-	+5.9/+15.4	+5.9/+15.4	-/-
50COF	765	2.6	0.0/0.0	-/-	0.0/0.0	-/-
50C50F	775	2.8	-0.6/+7.7	+1.3/+7.7	+1.3/+7.7	-/-
50C100F	800	3.0	-1.2/0.0	+4.6/+15.4	+4.6/+15.4	-/-
100COF	755	3.0	-1.3/+15.4	-/-	-1.3/+15.4	-/-
100C50F	760	3.2	-2.6/+23.1	+0.7/+6.7	-0.7/+23.1	-/-
100C100F	800	3.6	-1.2/+20.0	+6.0/+20.0	+4.6/+38.5	-/-
100C100FR	775	4.0	-/-	-/-	-/-	-3.1/+11.1

¹ Variation of slump flow/viscosity when adding coarse RCA to a mix with the same content of fine RCA and 0% coarse RCA

² Variation of slump flow/viscosity when adding fine RCA to a mix with 0% fine RCA and the same content of coarse RCA

³ Variation of slump flow/viscosity regarding the OCOF mix

⁴ Variation of slump flow/viscosity regarding the 100C100F mix

207 Since the effective w/c ratio was always equal to 0.50, all the mixes presented a slump flow between 700 and
 208 800 mm (Table 3), the objective defined in the mix design. Thus, the values of all hardened properties were
 209 comparable and only the effect of the different RCA fractions was analyzed [43]:

- Coarse RCA caused a minimal decrease in slump flow, always less than 3%, regardless of its content. However, it significantly increased viscosity t_{500} (around 20%), especially when 100% RCA was added. This result is explained by the irregular shape of RCA particles that enhanced friction between the SCC components [46].
- The use of fine RCA increased the slump flow by 1-6%. The negative effect of its irregular shape was balanced by its higher fines content than siliceous NA (Figure 1) [47]. Nevertheless, the irregular shaped particles worsened viscosity, which increased by around 15-20%, due to higher internal friction between the mix components [46].
- When adding fine RCA, the higher the content of coarse RCA, the less the slump flow increased compared to the slump flow of mix OCOF. Moreover, viscosity increases caused by each RCA fraction were higher when fine and coarse fractions were simultaneously used. Therefore, it appears that there was an interaction between both RCA fractions, due to the increased friction between the SCC components in both aggregate fractions.
- The more irregular shape of RCA powder 0-1 mm compared to limestone powder 0-1 mm also worsened both slump flow and viscosity.

225 Nevertheless, the worsening of the in-fresh behavior was lower than other results reported elsewhere in the
 226 literature [27, 42], which may be explained by the staged mixing process that maximized the water

227 absorption of RCA and, in turn, the flowability of the SCC [44].

228 **3.2. Mechanical performance**

229 **3.2.1. Compressive strength**

230 The main mechanical property of concrete is compressive strength, which was evaluated in the SCC mixes of
 231 this study at 7 and 28 days, as shown in Figure 4. In addition, trend lines regarding the effect of the addition
 232 of fine RCA for each coarse RCA content are also shown.

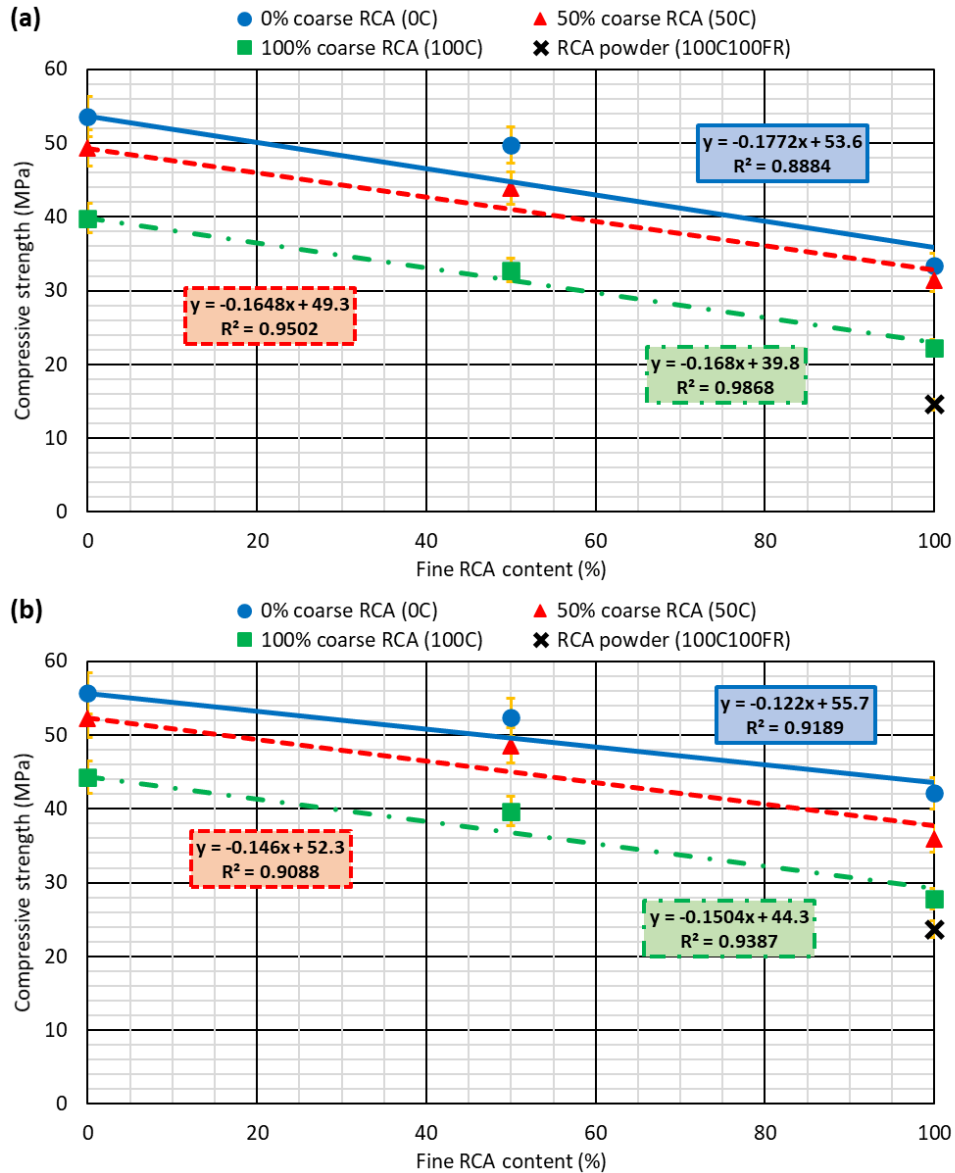


Figure 4. (a) 7-day compressive strength; (b) 28-day compressive strength

236 As expected, the addition of any RCA fraction decreased the compressive strength of SCC [30]. Thus, the
 237 compressive strength at 28 days of SCC with 100% NA was 55.7 MPa, while this property for SCC with 100%
 238 coarse, fine, and powder RCA presented a value of 23.7 MPa (57% compressive strength loss). The decrease
 239 of compressive strength caused by coarse RCA was attributed to the decrease of adhesion in the ITZ, due to

240 the adhered mortar [32] and to the lower strength of this waste compared to NA [48]. Regarding fine RCA,
241 the presence of altered mortar particles and the increased porosity of the cementitious matrix that it caused
242 (aspect shown in section 3.3) were the most detrimental aspects [49], which led to a higher decrease of
243 compressive strength than coarse RCA, as also shown in other studies [50, 51]. The use of RCA powder meant
244 extending the harmful effects of fine RCA to the powder fraction of the aggregate [47], which is necessary to
245 achieve adequate self-compactability, resulting in an even greater decrease in compressive strength.

246 In absolute values, the compressive strength reduction of SCC with the addition of a specific percentage of
247 coarse RCA was the same regardless of the content of fine RCA. So, the addition of 50% coarse RCA always
248 caused a reduction in the compressive strength at 28 days of 3-5 MPa, and 14-16 MPa for 100% coarse RCA.
249 Similarly, adding a certain amount of fine RCA resulted in a similar loss of compressive strength, regardless
250 of the coarse RCA content of the SCC. This trend is shown by the trend lines in Figure 4, which have similar
251 slopes at each age. In fact, the interaction p -value between both RCA fractions of the two-way ANOVA, Table
252 4, was higher than 0.05 (95% confidence level), which demonstrates that the interaction between both RCA
253 fractions was not significant. Thus, it can be stated that the effect of each RCA fraction was not influenced by
254 the added amount of the other RCA fraction and, therefore, the decrease in compressive strength caused by
255 the simultaneous addition of both fractions was statistically equal to the sum of the decreases separately
256 caused by each fraction [52].

257 Finally, with regard to the evolution of compressive strength over time, the addition of every RCA fraction
258 delayed the development of compressive strength. The reference mix 0C0F at 7 days had developed 96% of
259 its compressive strength at 28 days, while this value was only 90% and 79% for the mixes 100C0F and 0C100F,
260 respectively. Again, fine RCA had the most outstanding negative effect, and no interaction between the two
261 RCA fractions was found (Table 4). The negative effect of RCA powder was far greater, such that the
262 compressive strength at 7 days was only 61% of the 28-day compressive strength. This behavior might be
263 because of the higher internal curing of RCA compared to NA, due to its higher water absorption [53], which
264 leads to more noticeably delayed hydration of the cement [54]. This behavior caused that the decrease of
265 compressive strength when adding any RCA fraction was higher at 7 days than at 28 days.

266 **3.2.2. Modulus of elasticity**

267 The elastic stiffness of the mixes was defined by determining the modulus of elasticity at 7 and at 28 days,
268 whose values are depicted in Figure 5. As regards the compressive strength, both RCA fractions reduced the
269 modulus of elasticity of the SCC. This decrease at 28 days was 12% when adding 100% coarse RCA, 22% for
270 100% fine RCA, and 44% for 100% of both RCA fractions. The addition of 50% coarse RCA reduced the modulus
271 of elasticity by around 2% at 28 days, an almost negligible decrease, while 50% fine RCA caused a reduction
272 of 8-10%. Therefore, it is clear that fine RCA had a more detrimental effect than the coarse fraction, although

273 the most notable decrease occurred when adding RCA powder 0-1 mm (56% decrease in mix 100C100FR with
 274 respect to mix 0C0F), because this fraction concentrates the most negative effects of the fine fraction 0-4
 275 mm [55]. These decreases are in line with those obtained in other similar studies, in which decreases of 10-
 276 15% [51, 56] and 20-25% [50, 51] were obtained when adding 100% coarse and fine RCA, respectively. None
 277 of the RCA fractions affected the development of elastic stiffness over time, as the moduli of elasticity at 7
 278 days of all the mixtures were around 90% of their 28-day moduli of elasticity (two-way ANOVA, Table 4).

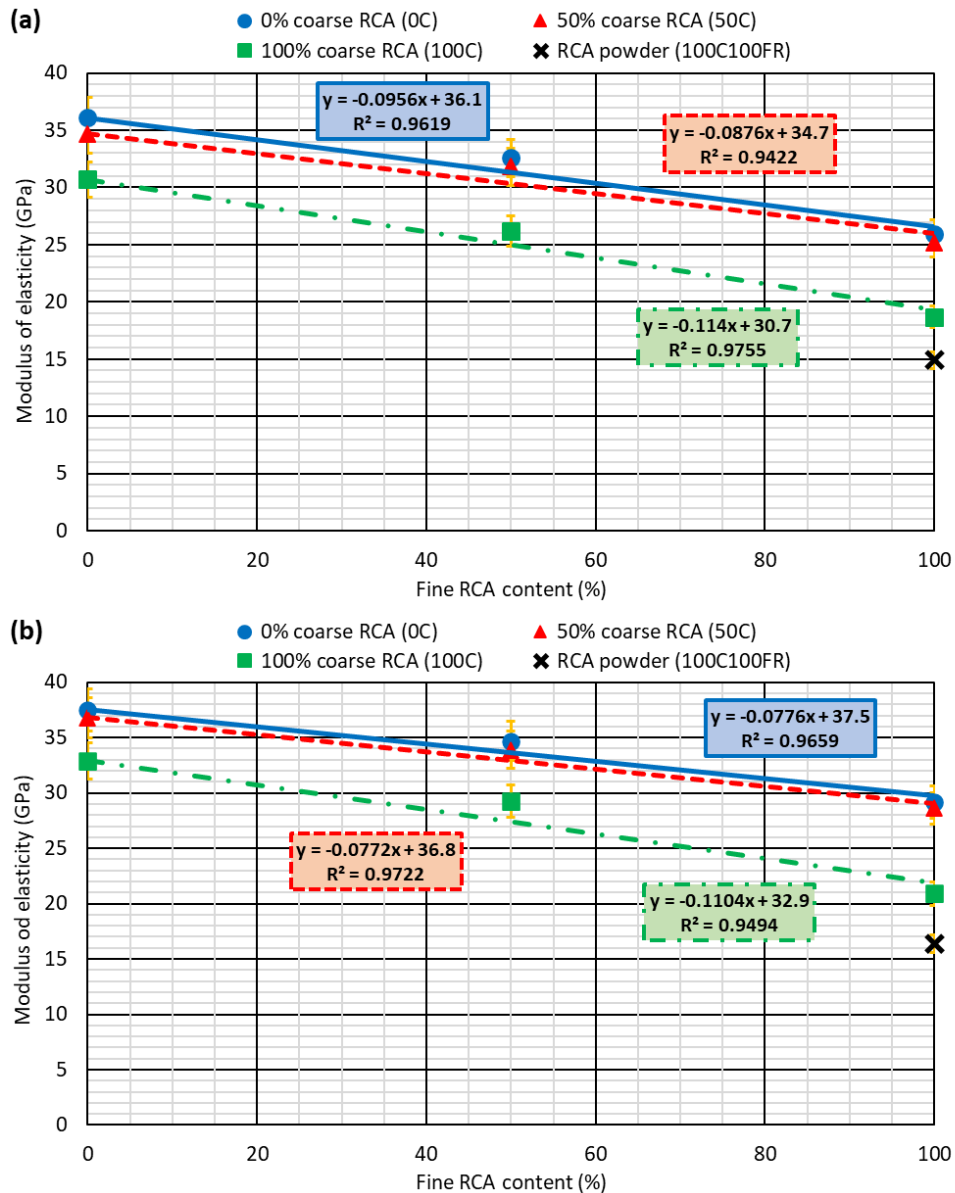


Figure 5. Modulus of elasticity at (a) 7 days; (b) 28 days

282 The two-way ANOVA values (Table 4) once again showed no interaction between both RCA fractions on the
 283 modulus of elasticity of SCC, so that the effects of both RCA fractions were independent of each other. This
 284 behavior has also been demonstrated in other similar studies in relation to both vibrated concrete and SCC
 285 [29, 42]. Alteration of this behavior was only observed in relation to the addition of increasing amounts of
 286 fine RCA to SCC with 100% coarse RCA. In these SCC mixes, the use of fine RCA led to a larger decrease in

287 elastic stiffness than in mixes with 0% or 50% coarse RCA (greater slope of the trend lines). However, this
 288 small increase was not enough for that interaction to be significant (p -value less than 0.05).

289 3.2.3. Splitting tensile strength

290 The addition of coarse RCA generally decreases adhesion within the ITZ, due to mortar adhering to the NA
 291 particles [29]. The application of tensile stresses therefore causes detachment between the cementitious
 292 matrix and the aggregate instead of the aggregate breaking [57]. The use of fine RCA generally increases
 293 these adhesion problems, amplifying the negative effect, as shown by microstructural analyses available in
 294 the literature [32]. These two effects mean that the use of any RCA fraction will decrease the splitting tensile
 295 strength [51], as observed in this study (Figure 6). Two relevant aspects can be observed in this figure:

- 296 • The decrease in splitting tensile strength when adding 50% coarse RCA was greater the higher the
 297 fine RCA content (6.1% between mixes 0C0F and 50C0F, and 15.8% between mixes 0C100F and
 298 50C100F). This behavior, shown by trend lines with increasing slopes (Figure 6), reflect a behavior
 299 that was attributed to the increase in adhesion problems when using both RCA fractions (two-way
 300 ANOVA, Table 4). However, no such behavior was observed between SCC with 50% and 100% coarse
 301 RCA, as any strength decrease was similar regardless of the added amount of fine RCA. Mixtures
 302 with 50% and 100% coarse and fine RCA were homogeneous groups in the two-way ANOVA.
- 304 • The mix prepared with 100% RCA in all fractions (100C100FR) showed the worst performance. The
 305 RCA powder accentuated the negative effects of fine RCA (altered mortar particles and increased
 306 porosity of the cementitious matrix) and so decreased concrete strength [47, 58]. This mix presented
 307 a splitting tensile strength of only 1.76 MPa, 58% lower than the strength of mix 0C0F.

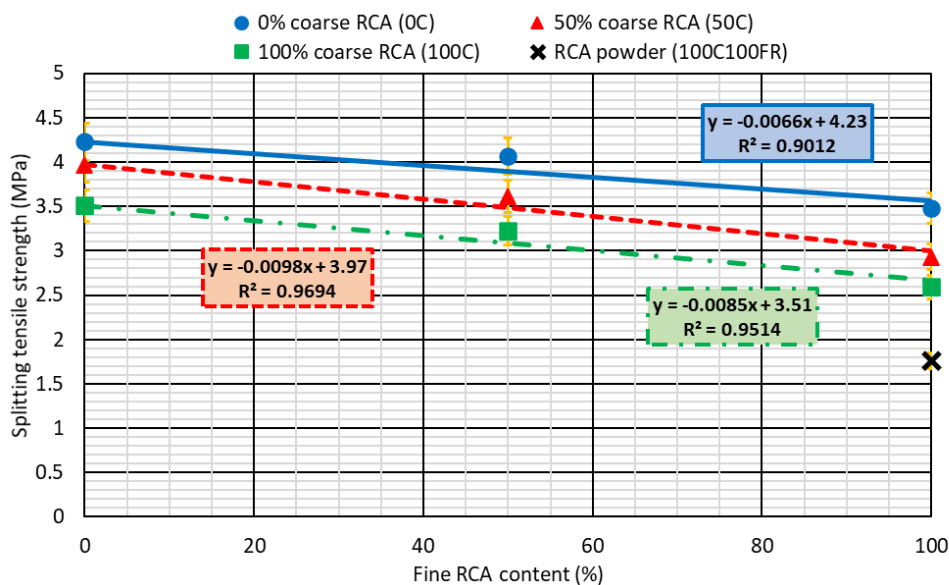


Figure 6. 28-day splitting tensile strength

310 **3.2.4. Flexural strength**

1

2 311 The effect of adding both RCA fractions on the flexural strength of SCC was very similar to the effect on the
3
4 312 modulus of elasticity and the compressive strength, as shown in Figure 7. The following may be mentioned:

5

6 313 • Both RCA fractions worsened the flexural strength of SCC. The addition of 100% of both fractions
7
8 314 caused practically the same strength decrease, as both mix 100C0F and mix 0C100F had flexural
9
10 315 strengths of 5.2-5.3 MPa, 15% lower than the flexural strength of the mix 0C0F. As in other studies,
11
12 316 regarding flexural strength, the decreased adhesion within the ITZ, due to the coarse RCA, was as
13
14 317 negative as the increased porosity, due to the fine RCA [27].

15 318 • No interaction between the two residue fractions was observed, as confirmed by the *p*-values of the
16
17 319 two-way ANOVA (Table 4). Thus, the decrease in flexural strength caused by the addition of any
18
19 320 coarse RCA content was very similar, regardless of the fine RCA content of the SCC. On the other
20
21 321 hand, the slope of the trend lines reflecting the strength decrease upon addition of fine RCA was
22
23 322 slightly greater with higher amounts of coarse RCA. However, this increasing strength decrease was
24
25 323 not high enough to be significant (Table 4), unlike the splitting tensile strength.

26 324 • The most damaging fraction for the mechanical behavior of SCC was the RCA powder, as mix
27
28 325 100C100FR presented a flexural strength of only 1.15 MPa, 70% and 81% lower than the flexural
29
30 326 strengths of mixes 100C100F and 0C0F, respectively.

31

32

33

34

35

36

37

38

39

40

41

42

43

44

45

46

47

48

49

50

51

52

53

54

55

56

57

58

59

60

61

62

63

64

65

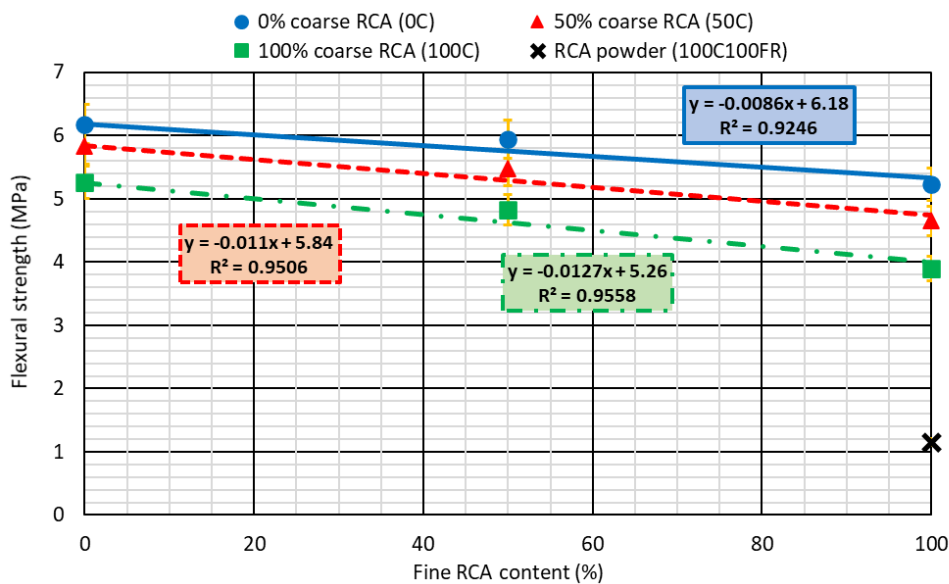


Figure 7. 28-day flexural strength

54 329 **3.2.5. Statistical significance**

55

56 330 The *p*-values for each factor (coarse RCA content and fine RCA content) and the factor's interaction of the
57
58 331 two-way ANalysis Of VAriance (ANOVA) for all the mechanical properties under evaluation are shown in Table
59
60 332 4. The content of both RCA fractions was always significant in the mechanical behavior, while the interaction

333 between both RCA fractions was significant only in the splitting tensile strength. Therefore, in general, the
 334 decrease of strength/stiffness caused by the simultaneous use of both RCA fractions was statistically equal
 335 to the sum of the decreases caused by each fraction individually [37].

Table 4. Two-way ANOVA of mechanical properties (significant values are those lower than 0.05)

Mechanical property	p-Value coarse RCA	p-Value fine RCA	p-Value interaction coarse and fine RCA
7-day compressive strength	0.0008	0.0003	0.1534
28-day compressive strength	0.0001	0.0001	0.2476
7-28 days compressive strength increase	0.0134	0.0394	0.3598
7-day modulus of elasticity	0.0006	0.0001	0.1756
28-day modulus of elasticity	0.0053	0.0013	0.0976
7-28 days modulus of elasticity increase	0.3532	0.0805	0.5673
28-day splitting tensile strength	0.0005	0.0003	0.0453 ¹
28-day flexural strength	0.0005	0.0004	0.0721

¹ Homogeneous groups: 50C0F and 100C0F; 50C50F and 100C50F; 50C100F and 100C100F

338 **3.3. Capillary-water-absorption test**

339 The capillary-water-absorption test allowed establishing the effective porosity of all the mixtures through
 340 the determination of water absorption of concrete [1]. Unlike other tests to determine porosity, such as the
 341 mercury intrusion porosimetry, this test is easy and cheap to perform [9], which is why it was chosen in this
 342 study.

343 **3.3.1 Water absorption**

344 The measurement of water absorption by capillarity was performed according to RILEM CPC 11.2 [45]. For
 345 this purpose, at 28 days, 100x100x100-mm cubic specimens were prepared in terms of humidity as per UNE
 346 83966 [59]. Subsequently, the skin was removed from one of their faces, which was placed in contact with a
 347 5±1 mm layer of water for 72 h, in order for the specimens to absorb water by capillary action. The four
 348 lateral faces of the specimens were waterproofed. During the test, the specimens were weighed at different
 349 time intervals depending on the time elapsed since the beginning of the test. Weighing was performed every
 350 hour at the beginning of the test, while at the end of the test, weighing was performed every 24 h.

351 The water absorption levels of the specimens throughout the test (72 h) are shown in Figure 8. The capillary
 352 water absorption of the SCC occurred at a higher rate during the first 6 h of the test, after which it slowed
 353 down, as shown by the lower slope of the graphs in Figure 8. This behavior is standard in concrete, such that
 354 capillary water absorption is very fast at the beginning of the test and it then stabilizes over time, once the
 355 pores closest to the absorption surface have been saturated [8, 10]. On the other hand, the relationship
 356 between 72-h water absorption and coarse and/or fine RCA content is shown in Figure 9, for an easier
 357 comparison of water absorption of the mixtures. It can be seen that an increase in the content of either RCA
 358 fraction led to an increase in capillary water absorption, due to the increase in concrete porosity caused by
 359 this residue, because of the need to increase the w/c ratio when adding it to maintain the flowability of the
 360 SCC [60], as well as the worse affinity of this waste with the other concrete components [28].

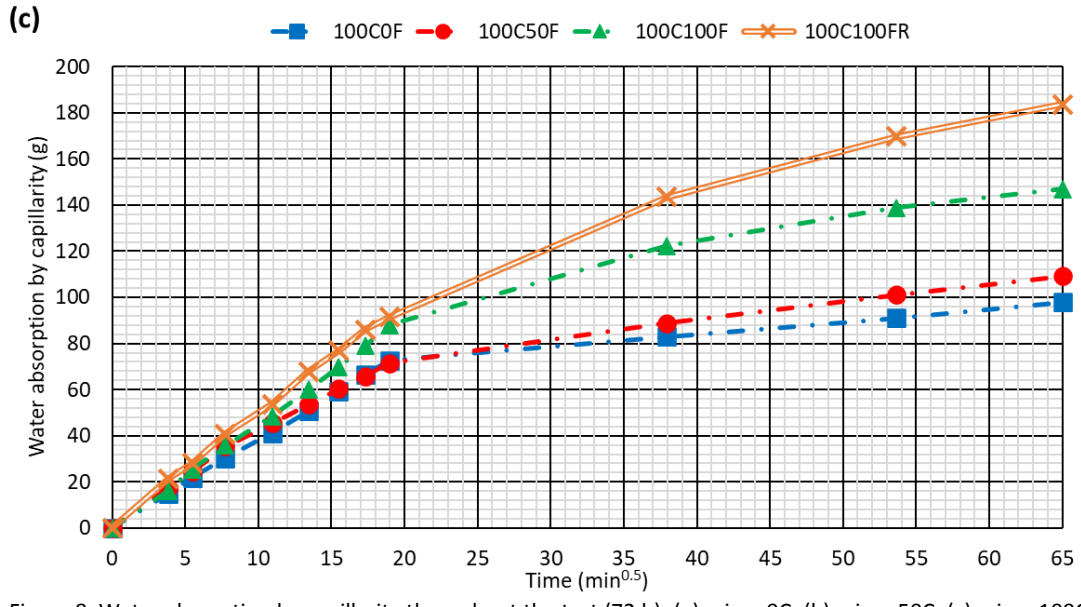
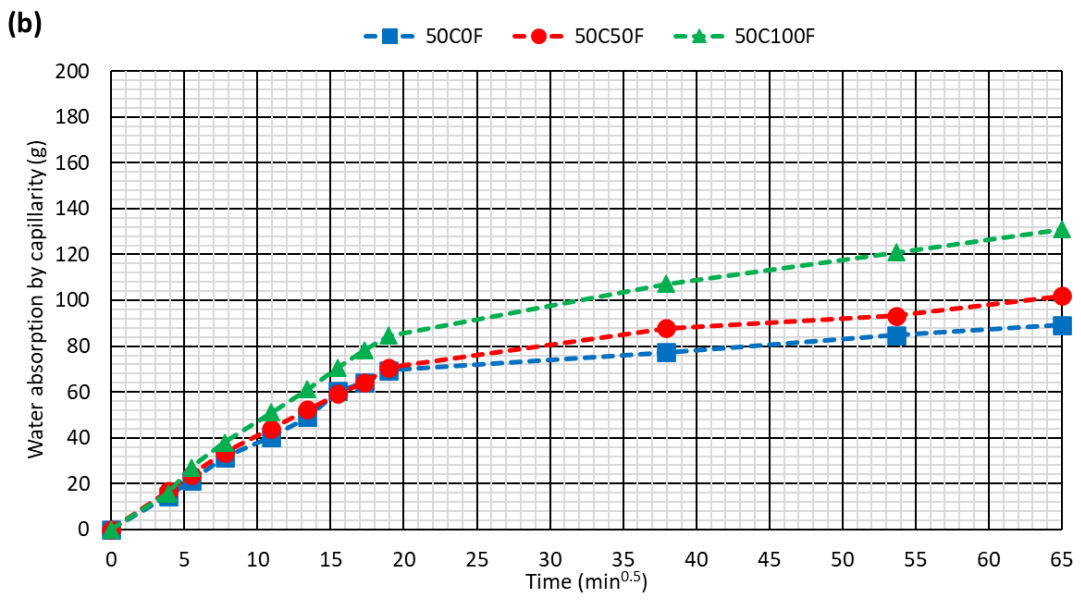
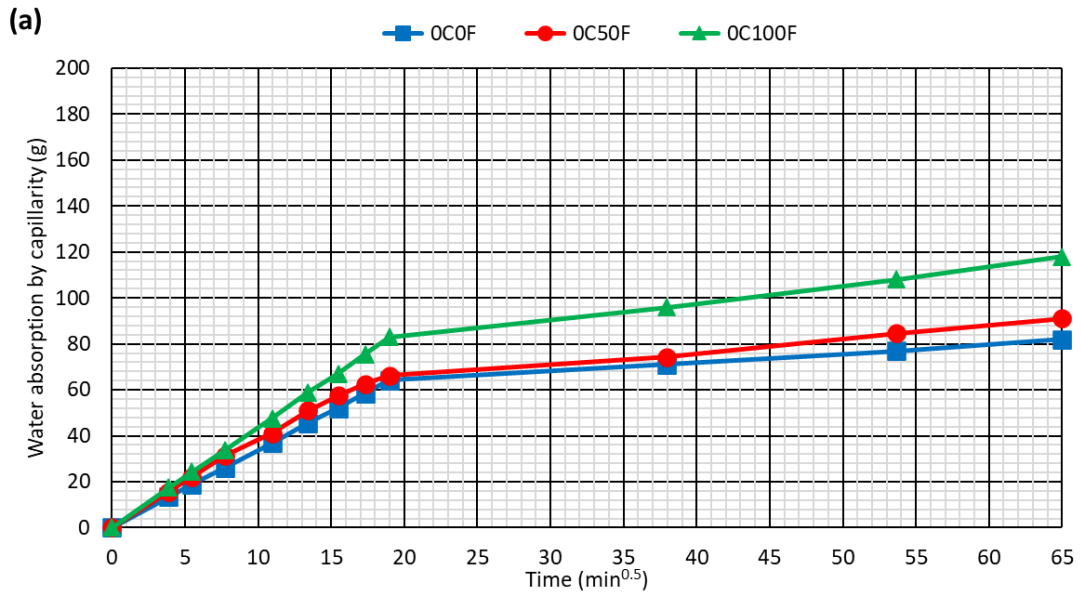


Figure 8. Water absorption by capillarity throughout the test (72 h): (a) mixes OC; (b) mixes 50C; (c) mixes 100C

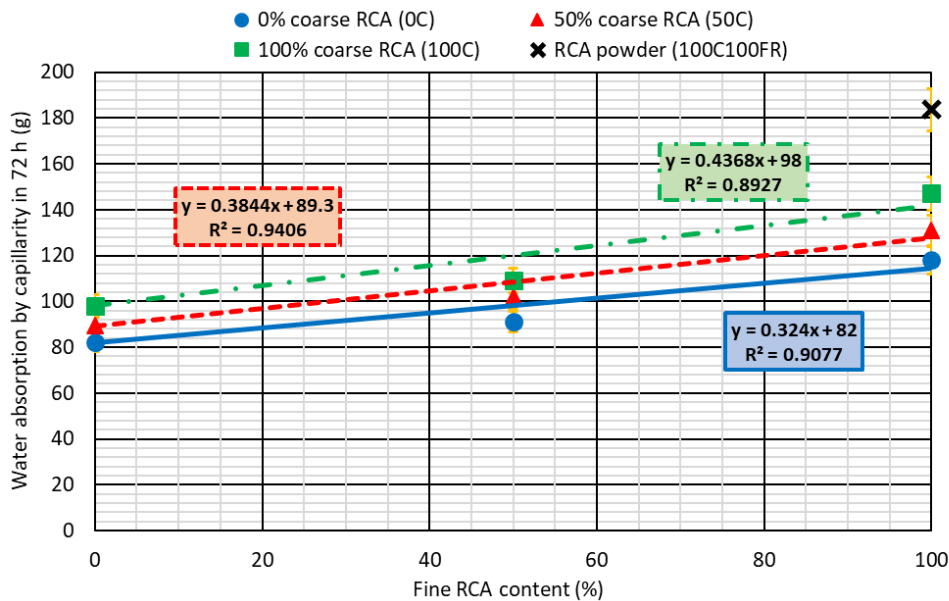


Figure 9. Relationship between water absorption by capillarity in 72 h and fine RCA content

In Figure 8 and Figure 9, the following aspects can be noted in relation to the effects of the different RCA fractions on the capillary water absorption of SCC:

- The increase in 72-h water absorption was greater when fine RCA was added (Figure 9). Thus, the addition of 100% coarse RCA led to a 20% increase in capillary water absorption within 72 h, while the increase was 44% after having added 100% fine RCA. These results are in line with those shown in the literature, according to which the addition of the same amount of fine as coarse RCA generally results in twice the increase in long-term water absorption when the fine fraction is used [61].
- The increase in 72-h water absorption with increased additions of fine RCA showed a linear trend, but this water absorption was lower than expected with the addition of 50% fine RCA. Furthermore, the slope of the trend line of the 72-h water absorption as a function of fine RCA content was greater the higher the coarse RCA content of SCC, as shown in Figure 9. In the same figure, it is shown that the increased water absorption in 72 h, caused by an increasing content of coarse RCA, was similar in the SCC mixes with 0% and 50% fine RCA, but 60% higher in mixes 100F. It can therefore be stated that there was an interaction between both RCA fractions, as confirmed by the *p*-value of interaction (0.03271) obtained in the two-way ANOVA. As reported in other studies in relation to conventional vibrated concrete [61], the increase in porosity, which conditions water absorption by capillarity, was amplified by simultaneously increasing the content of both RCA fractions; their combined effect exceeding the sum of the effect of using each RCA fraction individually [27].
- The effect of both RCA fractions was perceptible 6 h after the start of the test. As can be seen in Figure 8, the mixtures with 0% and 50% fine RCA and the same coarse RCA content presented very similar water absorption levels during the initial 6h of testing, with only one notable difference in this period of time when adding 100% fine RCA. The same occurred when adding coarse RCA, as the

389 SCC with the same fine RCA content and different coarse RCA contents showed no notable difference
 390 at the start of the test. Therefore, the really comparable values were those at 6 h after the start of
 391 the test (Figure 9) [45, 62], on which the statements of the two previous bullet points are based.
 392 • Powder 0-1 mm of this residue was the fraction that had the most unfavorable effect, in line with the
 393 mechanical behavior, as demonstrated by mix 100C100FR. Its addition doubled the increase in water
 394 absorption caused by adding 100% fine RCA 0-4 mm and its use is therefore not recommendable.

395 **3.3.2. Permeation coefficient and sorptivity**

396 There are basically two mathematical equations that model the capillary water absorption of concrete. Each
 397 model provides a parameter that defines the rate at which the concrete absorbs water by capillary action.
 398 Both parameters are important in terms of durability, as they show how easily dangerous external agents
 399 can penetrate into concrete [10].

400 • On the one hand, the Fangerlund model [62], which assumes that water absorption by capillarity of
 401 concrete is a linear function of the square root of time. The slope of the aforementioned straight line
 402 expressed per unit area, so that this coefficient is not influenced by the size of the test specimen, is
 403 called the permeation coefficient, K , expressed in $\text{g}/(\text{m}^2 \cdot \text{min}^{0.5})$. This coefficient is calculated by
 404 Equation 1, in which ΔM is the increased mass of the specimen due to the absorption of water by
 405 capillarity in g; A , the exposed area in m^2 ; and t , the time in minutes. The most representative straight
 406 section of the graphic of the test must be considered to calculate this coefficient (Figure 8), *i.e.*, the
 407 time period from 6 h to 72 h when the results of the test are fully comparable [45, 62], as was
 408 explained in the previous section.

$$K = \frac{\Delta M}{A \times \Delta\sqrt{t}} \quad (1)$$

409 • On the other hand, the Hall model is based on the assumption that water absorption by capillarity is
 410 adjusted by a combination of functions dependent on the first power of time and the square root of
 411 time [63], as shown in Equation 2. In this expression, ΔM_u is the increase in mass due to water
 412 absorption by capillarity in g/m^2 ; t , the time in minutes; S , the sorptivity in $\text{g}/(\text{m}^2 \cdot \text{min}^{0.5})$; and A and
 413 B , adjustment coefficients. Sorptivity can be calculated by fitting this model to the experimental
 414 results obtained through multiple regression [37]. Sorptivity is therefore more complicated to
 415 determine than the permeation coefficient.
 416

$$\Delta M_u = A + S \times \sqrt{t} - B \times t \quad (2)$$

417 Both the permeation coefficient, K , and the sorptivity, S , of each mixture is shown in Table 5. It can be
 418 observed that the higher the water absorption during the test (Figure 8 and Figure 9), the higher the value of
 419 these coefficients. Higher water absorption levels are not only linked to an increase in porosity, but also to a

421 larger pore size and higher inter-pore connectivity, so that water can penetrate faster [14, 64], increasing the
 422 values of these parameters [63]. Therefore, the higher the content of RCA in SCC, the higher the capillary-
 423 water-absorption rate, as also reported in the literature [8].

Table 5. Permeation coefficient, K ; sorptivity, S ; and accessible porosity of the mixes

Mix	Permeation coefficient K ($\text{g}/\text{m}^2\cdot\text{min}^{0.5}$)	Sorptivity S ($\text{g}/\text{m}^2\cdot\text{min}^{0.5}$)	R^2 Hall model adjustment (%)	Accessible porosity (%)
OC0F	38.1	2617	94.85	8.2
OC50F	53.0	2669	94.44	9.1
OC100F	75.1	3354	96.07	11.8
50C0F	42.6	2731	94.62	8.9
50C50F	67.0	2767	97.06	10.2
50C100F	99.5	3582	97.65	13.1
100C0F	54.1	2923	95.70	9.8
100C50F	80.9	2965	97.35	10.9
100C100F	126.3	3882	99.25	14.7
100C100FR	197.2	4149	99.81	18.4

425 Sorptivity was notably higher than the permeation coefficient because the calculation of this last coefficient
 426 gives no consideration to the first 6 h of the test. For the same reason, the permeation coefficient had a
 427 higher relative increase than sorptivity following the addition of RCA. The increase of both coefficients was
 428 much greater when adding fine RCA, due to the greater increase in water absorption caused by this fraction
 429 of RCA [34]. Considering the percentages of added RCA, it can be observed that in a mixture with a certain
 430 content of coarse RCA (0%, 50% or 100%), the addition of 50% fine RCA resulted in a small increase in the
 431 permeation coefficient and sorptivity compared to that caused by the addition of 100% fine RCA (Table 5).
 432 Similarly, in the SCC mixes with a certain fine RCA content, the addition of 50% coarse RCA resulted in a
 433 smaller increase in both coefficients than adding 100% coarse RCA. These effects have also been observed
 434 when adding aggregates of similar nature in vibrated concrete [63] and may be explained by the interactions
 435 between both RCA fractions regarding water absorption by capillarity explained in the previous section.
 436 Finally, in spite of all the above, the coefficients of mix 100C100FR, manufactured with RCA powder, were
 437 the highest, probably due to the larger size of its pores, in which the water could penetrate faster [57].

438 Concrete durability may be analyzed with these coefficients [1, 9]. In general, for instance, permeation
 439 coefficients lower than $35 \text{ g}/(\text{m}^2\cdot\text{min}^{0.5})$ correspond to high-quality concrete mixtures; if the value exceeds
 440 $100 \text{ g}/(\text{m}^2\cdot\text{min}^{0.5})$, the quality of concrete is qualified as poor due to the risk of easy penetration of external
 441 harmful agents, such as sulphates and chlorides [10]. The results obtained were in line with the values of
 442 similar studies in the literature [27], so that all the mixtures presented an intermediate durable quality, with
 443 a permeation coefficient between 35 and $100 \text{ g}/(\text{m}^2\cdot\text{min}^{0.5})$. Only mixes 100C100F and 100C100FR could
 444 present durability problems (poor durable quality, permeation coefficient higher than $100 \text{ g}/(\text{m}^2\cdot\text{min}^{0.5})$), due
 445 to the accessibility of aggressive external agents [16].

446 **3.3.3. Effective (accessible) porosity**

447 Water absorption by capillarity over 72 h, which is fast and easy to perform, provides a coarse estimation of
448 the effective (accessible) porosity of concrete [8]. According to both the Fangerlund and the Hall models [62,
449 63], the porosity of the mixtures can be calculated according to Equation 3, in which ε_e is the accessible
450 porosity (interconnected pores) of the mixture as a percentage (%); ΔM , the total mass increase over the 72
451 h of the specimen, due to water absorption by capillarity in g; V , the volume of the specimen in cm^3 ; and ρ ,
452 the water density (1 g/cm^3).

$$\varepsilon_e = \frac{\Delta M}{V \times \rho} \times 100 \quad (3)$$

454 The effective porosity values are shown in the fourth column of Table 5. As expected, the results were in
455 accordance with the water absorption and water-absorption-rate coefficients [62, 63]. Thus, the fine RCA
456 caused a greater increase in porosity than the coarse RCA, as the reference mix, mix 0C0F, presented an
457 effective porosity of 8.2%, and mixes 100C0F and 0C100F of 9.8% and 11.8%, respectively. Moreover, porosity
458 following the addition of 50% of any RCA fraction increased less than expected according to the effective
459 porosity when adding 100%. Behavior that reflects the aforementioned interaction between both RCA
460 fractions.

461 **3.3.4. Effective porosity estimation**

462 The porosity of concrete prepared with NA is linked to the amount of free (effective) water, *i.e.*, the water
463 that is not absorbed by the aggregate of the concrete mix [5, 10]. In case alternative materials, such as RCA,
464 are added, the affinity between them and the rest of the concrete components also conditions this property
465 [33]. Therefore, both aspects have to be considered in any estimation of concrete porosity.

466 The effective w/c ratio remained constant in the SCC mixes of this study, for the calculation of which the
467 water absorption within 15 minutes (mixing time) of the aggregates was considered (Table 1). This implied
468 that, since all the mixes had the same amount of cement, the free water after 15 minutes of mixing was the
469 same in all the mixes. Nevertheless, the porosity was completely different in all of them (Table 5), which
470 reveals the relevance of the affinity between the different concrete components. It is therefore necessary to
471 look for a variable that shows the influence of the water added to the mixture and also, indirectly, the
472 aforementioned affinity.

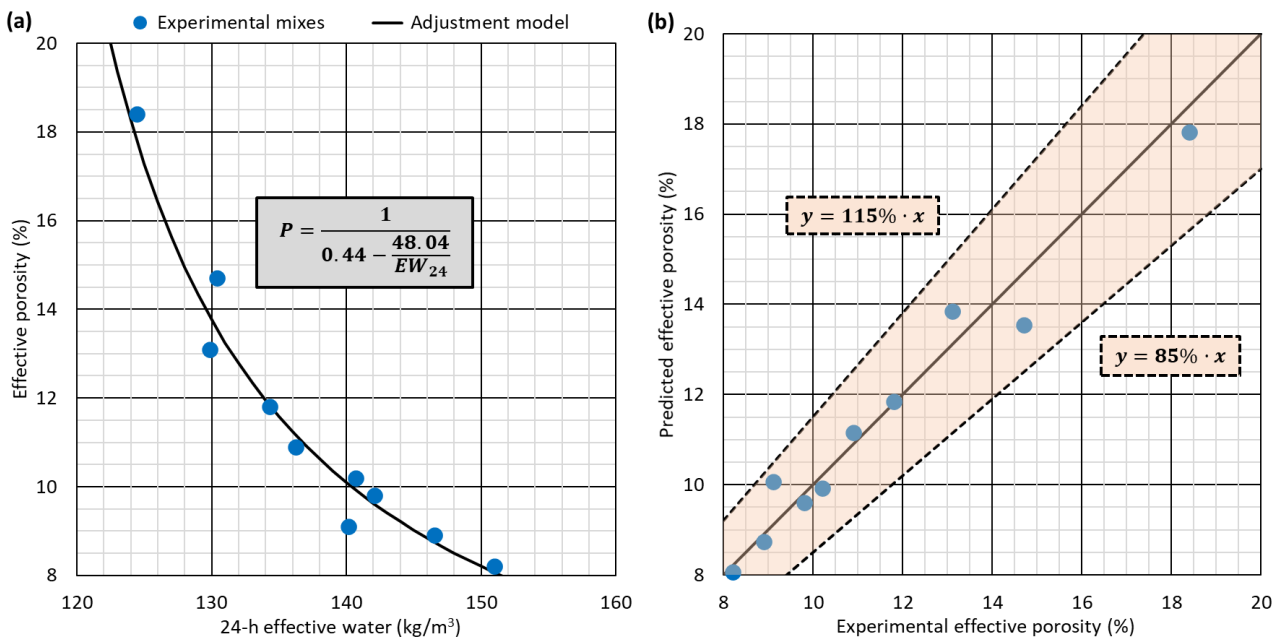
473 After different attempts, it was found that the effective water at 24 h, which has no real physical meaning,
474 since at 24 h the concrete has already hardened, fulfilled both requirements. On the one hand, it reflected
475 the variation of the amount of water added when incorporating RCA to maintain the workability of SCC [42].
476 On the other, the large difference in 24-h water absorption between NA and RCA and between both RCA
477 fractions [39] proved to be a variable that statistically reflected the affinity of RCA with the other SCC

478 components. This magnitude can be calculated according to Equation 4, in which EW_{24} is the 24-h effective
 479 water in kg/m^3 ; W , the water added to the concrete in kg/m^3 ; $WA_{24,i}$, the 24-h water absorption of each
 480 aggregate in percentage; and AA_i , the added amount of each aggregate in kg/m^3 .

$$EW_{24} = W - \sum_i \left(\frac{WA_{24,i}}{100} \times AA_i \right) \quad (4)$$

482 The performance of a simple regression between the 24-h effective water (EW_{24} , kg/m^3) and the effective
 483 porosity (P , %) showed that both magnitudes were related to each other with a double reciprocal model and
 484 a high coefficient R^2 (95.36%). This model, shown in Equation 5 and depicted in Figure 10a, was used to
 485 estimate the effective porosity of the mixtures with a maximum deviation of 15% with respect to the
 486 experimental value, as shown in Figure 10b.

$$P = \frac{1}{0.44 - \frac{48.04}{EW_{24}}} \quad (5)$$



488
 489 Figure 10. (a) Simple-regression model between 24-h effective water and effective porosity; (b) Relationship between experimental
 490 and predicted effective porosity

491 The porosity of concrete is undoubtedly linked to its composition, as has been clearly shown in this section.
 492 In addition to the inclusion of alternative materials, porosity is likewise conditioned by the cement content,
 493 the aggregate-to-cement ratio and the type and amount of admixture in use [14, 16]. The model presented
 494 in Equation 5 is therefore only valid for an SCC of a similar composition to the one in this research work,
 495 which has standard amounts of all components, *i.e.*, the SCC concrete developed in this study can be
 496 considered conventional. A statistical adjustment of the results of mixtures with different (vibrated,
 497 pumpable, and self-compacting) types of workability and composition will be needed to formulate a more

498 generic expression.

499 **3.5. Estimation of mechanical properties through porosity**

500 Different studies in the literature have reported models for estimating the mechanical properties of concrete
 501 with RCA [29, 37, 65]. These models generally vary depending on the fraction of RCA that is added. In this
 502 section, the aim is to show the usefulness of porosity for estimating the mechanical properties of concrete,
 503 regardless of the RCA fraction in use. In addition, models for estimating the mechanical behavior of
 504 conventional SCC are also provided.

505 **3.5.1. Simple regression**

506 Table 6 shows the simple-regression models that allow the most accurate estimation of the mechanical
 507 properties of the mixtures as a function of their porosity (P , in percent %). In addition, the expressions that
 508 provide the minimum expected value of each mechanical property at a confidence level of 95% are also
 509 included. Maximization of the coefficient R^2 was performed to obtain all these expressions.

Table 6. Simple-regression models between porosity and mechanical properties

Property	Simple-regression adjustment model	Minimum expected value formula	Coefficient R^2 (%)
Compressive strength at 7 days (CS_7 , MPa)	$CS_7 = 1/(0.00564 + 0.00018 \times P^2)$	$CS_7^{min} = \exp(6.11 - 0.81 \times \sqrt{P})$	97.78
Compressive strength at 28 days (CS_{28} , MPa)	$CS_{28} = 1/(0.012220 + 0.000093 \times P^2)$	$CS_{28}^{min} = \exp(5.57 - 0.58 \times \sqrt{P})$	95.44
Modulus of elasticity at 7 days (ME_7 , GPa)	$ME_7 = 1/(0.01790 + 0.00015 \times P^2)$	$ME_7^{min} = \exp(5.36 - 0.63 \times \sqrt{P})$	97.24
Modulus of elasticity at 28 days (ME_{28} , GPa)	$ME_{28} = 1/(0.01731 + 0.00013 \times P^2)$	$ME_{28}^{min} = \exp(5.35 - 0.60 \times \sqrt{P})$	96.82
Splitting tensile strength at 28 days (STS_{28} , MPa)	$STS_{28} = 1/(0.1532 + 0.0012 \times P^2)$	$STS_{28}^{min} = \exp(2.94 - 0.56 \times \sqrt{P})$	97.16
Flexural strength at 28 days (FS_{28} , MPa)	$FS_{28} = 7.288 - 0.017 \times P^2$	$FS_{28}^{min} = 6.770 - 0.018 \times P^2$	96.16

511 It can be observed that the optimal relationship between porosity and those mechanical properties that
 512 depend on the application of a single type of stress -compression (compressive strength and modulus of
 513 elasticity) or tensile (splitting tensile strength)- was always of the same nature. In other words, the
 514 adjustment model always corresponded to the expression of Equation 6 (MP , mechanical property; P ,
 515 porosity), while only the adjustment coefficients a and b varied. It was also reflected in the expression for
 516 the determination of the minimum expected value of the different mechanical properties, since this
 517 expression always responded to Equation 7 (MP^{min} , minimum expected value of the mechanical property; P ,
 518 porosity), once again varying only the adjustment coefficients a and b . The flexural strength, which depends
 519 on the compressive and tensile behavior of the concrete, presented expressions of a different nature.

$$MP = \frac{1}{a + b \times P^2} \quad (6)$$

$$MP^{min} = \exp(a - b \times \sqrt{P}) \quad (7)$$

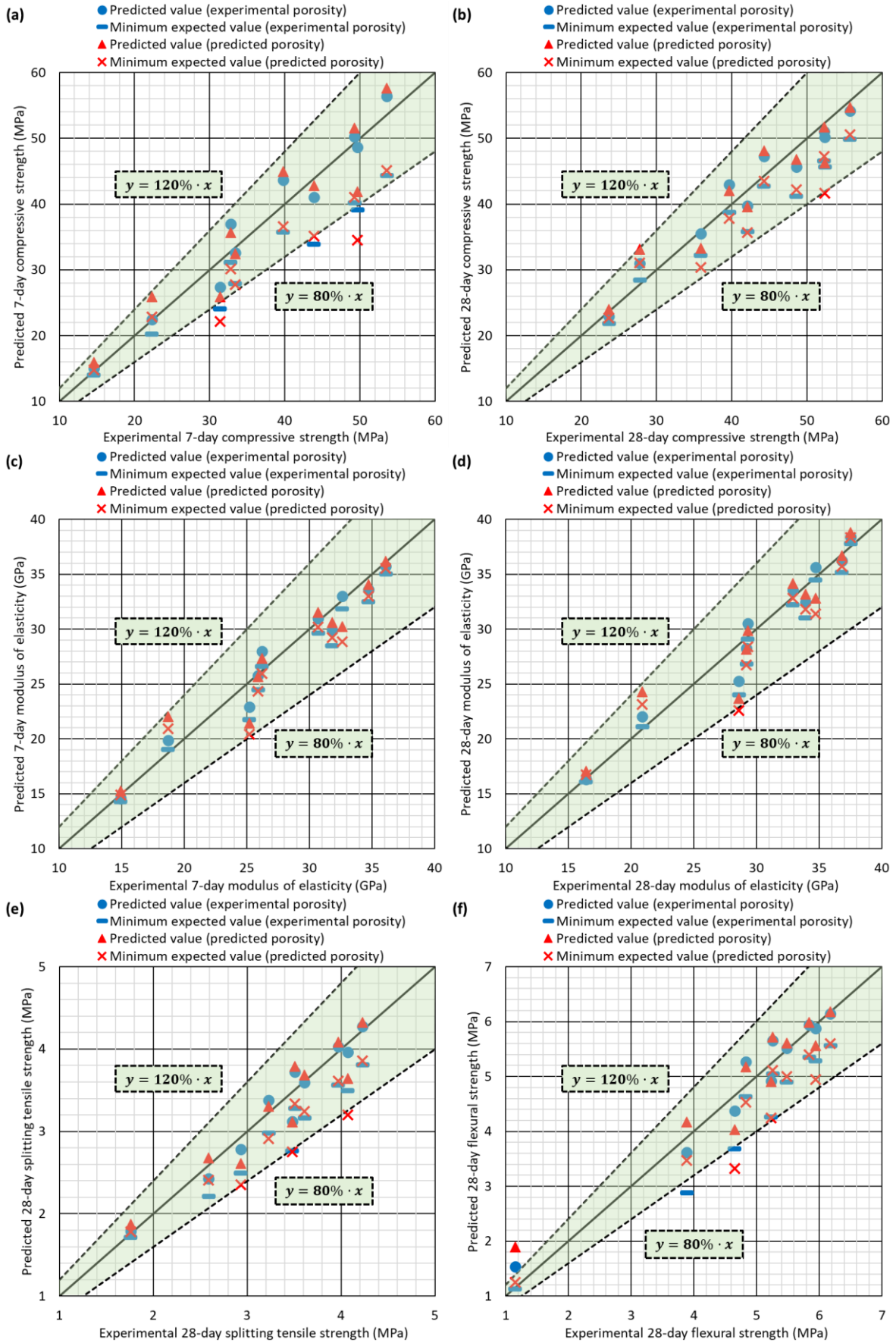


Figure 11. Comparison between experimental and predicted mechanical properties using simple-regression models: (a) 7-day compressive strength; (b) 28-day compressive strength; (c) 7-day modulus of elasticity; (d) 28-day modulus of elasticity; (e) 28-day splitting tensile strength; (f) 28-day flexural strength

528 Figure 11 shows the comparison between the experimental values of all the mechanical properties and the
529 value predicted through the models listed in Table 6. For each experimental value, four values calculated
530 using these models were provided: the mechanical property estimated through the experimental porosity,
531 the mechanical property estimated from the porosity calculated using the 24-h effective water (Equation 5),
532 the minimum value of the mechanical property calculated using the experimentally determined porosity, and
533 the minimum value of the mechanical property obtained from the estimated porosity (Equation 5). The
534 accuracy of the model can be seen in its estimates of the mechanical behavior of SCC, because of the
535 following reasons, which also underline the usefulness of the porosity as estimated in Equation 5:

- 536 • Regardless of the porosity under consideration, whether experimental or estimated, the estimated
537 value of the mechanical property never varied by more than $\pm 20\%$ from the experimental value,
538 which is a reasonable level of accuracy. Only the flexural strength of mix 100C100FR (Figure 11f)
539 never met this aspect, due to the remarkably low experimental value (1.15 MPa).
- 540 • In general, the estimated value of the mechanical property was lower than the experimental value.
541 This situation occurred more frequently when the experimentally measured porosity was used. It
542 shows that in most cases the proposed models never overestimated the mechanical property. When
543 the mechanical property was overestimated, this overestimation was on average lower than 15%.
544 The values obtained with these models could therefore be safely used in structural design [41, 66].
- 545 • Obviously, the minimum expected value was always lower than the predicted one and provided an
546 adequate safety margin in all cases. But in addition, the minimum expected value was always lower
547 than the experimental value except for 5 out of 60 times (8% of the times). Therefore, the minimum
548 expected value can be considered an adequate estimation of the mechanical property from a safety-
549 theory point of view [41, 66]. This trend was obtained regardless of whether the experimental or
550 estimated porosity levels were used.

551 **3.5.2. Multiple regression**

552 The estimation of the mechanical properties of SCC with RCA through porosity levels can be performed
553 reliably and safely, as shown in the previous section. However, the porosity of the mixtures must be correctly
554 determined or an accurate equation for its estimation must be established, such as the one obtained in this
555 study (Equation 5). Incorrect moisture conditioning of the test specimens, or an excess/defect of the height
556 of the water layer when performing the capillary-water-absorption test could lead to incorrect porosity
557 values [1, 9]. It implies that the application of the simple-regression models (Table 6) might result in an
558 incorrect estimation of the mechanical properties of the SCC, despite their high accuracy. One way of avoiding
559 this problem is to complement porosity with another property of the concrete, so that multiple-regression
560 models may be used to estimate the mechanical properties. In this way, even if the value of porosity is not

561 correct, the error in the estimation of the mechanical property will be much smaller, because the second
 562 prediction property will help to maintain predictive accuracy [37].

563 Compressive strength is the most commonly and easily measured mechanical property in commercially
 564 produced concrete [35]. In addition, there is traditionally a trend to relate it to the rest of the mechanical
 565 properties, as shown by the formulas contained in international standards such as Eurocode 2 [41] or ACI-
 566 318 [66]. For these reasons, it was decided to develop multiple-regression models in which the estimation of
 567 the SCC mechanical properties was based on the porosity and compressive strength of the mixtures. This
 568 approach follows the traditional trend and provides greater robustness to the estimation of the mechanical
 569 behavior of SCC based on porosity, while disregarding the RCA fraction and amount in use. Simple-regression
 570 models with compressive strength as the only prediction variable have been shown to depend on the RCA
 571 fraction used to produce the concrete [29, 65]. However, using multiple-regression models implies that the
 572 estimation of compressive strength can only be performed through simple-regression models (Table 6).

573 The development of simple-regression models between the different mechanical properties and the
 574 compressive strength showed that the relationship regarding the modulus of elasticity and splitting tensile
 575 strength could be optimally adjusted, by RCA fractions, to Equation 8 (*MP*, mechanical property, modulus of
 576 elasticity and splitting tensile strength; *CS*, compressive strength), varying only the adjustment coefficients
 577 (*a* and *b*). Therefore, the trend shown by the simple regression between these properties and porosity was
 578 maintained, in which the optimal model was always similar for those mechanical properties that depended
 579 on a single type of stress. Likewise, the optimal simple-regression model by RCA fractions for flexural strength
 580 presented a different expression (Equation 9; *FS*, flexural strength).

$$MP = (a + b \times \ln(CS))^2 \quad (8)$$

$$FS = \sqrt{a + b \times \ln(CS)} \quad (9)$$

Table 7. Multiple-regression models between porosity, compressive strength and mechanical properties

Property	Multiple-regression adjustment model	Coefficient R ² (%)
7-day modulus of elasticity (<i>ME</i> ₇ , in GPa)	$ME_7 = \frac{(1.0984 + 3.0593 \times \ln(CS_7))^2}{4.6140 + 0.0049 \times P^2}$	98.54
28-day modulus of elasticity (<i>ME</i> ₂₈ , in GPa)	$ME_{28} = \frac{(-0.12354 + 0.85469 \times \ln(CS_{28}))^2}{0.26555 + 0.00036 \times P^2}$	97.78
Modulus of elasticity regardless of age (<i>ME</i> , in GPa)	$ME = \frac{(0.45129 + 0.94915 \times \ln(CS))^2}{0.44396 + 0.00069 \times P^2}$	97.75
28-day splitting tensile strength (<i>STS</i> ₂₈ , in MPa)	$STS_{28} = \frac{(0.233 + 1.645 \times \ln(CS_{28}))^2}{10.094 + 0.016 \times P^2}$	97.58
28-day flexural strength (<i>FS</i> ₂₈ , in MPa)	$FS_{28} = (\sqrt{93.5503 - 10.2686 \times \ln(CS_{28})}) \times (1.0015 - 0.0024 \times P^2)$	96.35

584 By combining the expressions of the simple-regression models between porosity and mechanical properties,

585 and between compressive strength and mechanical properties, the models shown in Table 7 (P , porosity in
 586 %; CS_7 , 7-day compressive strength in MPa; CS_{28} , 28-day compressive strength in MPa; CS , compressive
 587 strength regardless of age) were obtained. It can be observed that the coefficient R^2 of all the models was
 588 very high, over 96% in all cases, which shows the accuracy of the models under development. Furthermore,
 589 in Table 8, the formulas to calculate the minimum expected value at a confidence level of 95% through
 590 multiple regression are shown. The formulas for calculating the minimum expected value were of the same
 591 nature (same mathematical expression but with different adjustment coefficients) as the estimation models
 592 (Table 7).

Table 8. Multiple-regression models between porosity, compressive strength, and mechanical properties

Property	Minimum expected value formula
7-day modulus of elasticity (ME_7 , in GPa)	$ME_7 = \frac{(-0.31912 + 0.85140 \times \ln(CS_7))^2}{0.26860 + 0.00026 \times P^2}$
28-day modulus of elasticity (ME_{28} , in GPa)	$ME_{28} = \frac{(-0.43389 + 0.72480 \times \ln(CS_{28}))^2}{0.15811 + 0.00029 \times P^2}$
Modulus of elasticity regardless of age (ME , in GPa)	$ME = \frac{(-0.00052 + 0.66913 \times \ln(CS))^2}{0.18546 + 0.00033 \times P^2}$
28-day splitting tensile strength (STS_{28} , in MPa)	$STS_{28} = \frac{(-0.0778 + 0.8970 \times \ln(CS_{28}))^2}{2.7811 + 0.0070 \times P^2}$
28-day flexural strength (FS_{28} , in MPa)	$FS_{28} = (\sqrt{75.7772 - 5.5062 \times \ln(CS_{28})}) \times (0.8931 - 0.0024 \times P^2)$

594 Figure 12 shows the comparison between the experimental value of the different mechanical properties and
 595 the value estimated through the multiple-regression models. Furthermore, the minimum expected value is
 596 also shown. The following three aspects should therefore be emphasized:

- The estimation provided by the multiple-regression models, with deviation values of $\pm 10\%$ with respect to the experimental value, was much more accurate than the results of the simple-regression models. The flexural strength of mix 100C100FR never met this requirement, due to the very low experimental value obtained. Against the multiple-regression models is their greater complexity, making their application slightly more difficult than that of the simple-regression models [37].
- The estimation was equally correct regardless of whether the experimentally measured porosity or the porosity estimated through Equation 5 was used. In fact, the values of the mechanical properties calculated with each porosity differed from each other by 5% on average, lower than the 12% of the simple-regression models (Figure 11). An accuracy level that was due to the introduction of compressive strength as a second variable, which reduced the estimation dependence on porosity.
- The minimum expected value of the mechanical properties was always lower than the experimental one, regardless of the porosity levels, whether experimentally measured or predicted. Therefore, the use of the minimum expected value was always on the safe side.

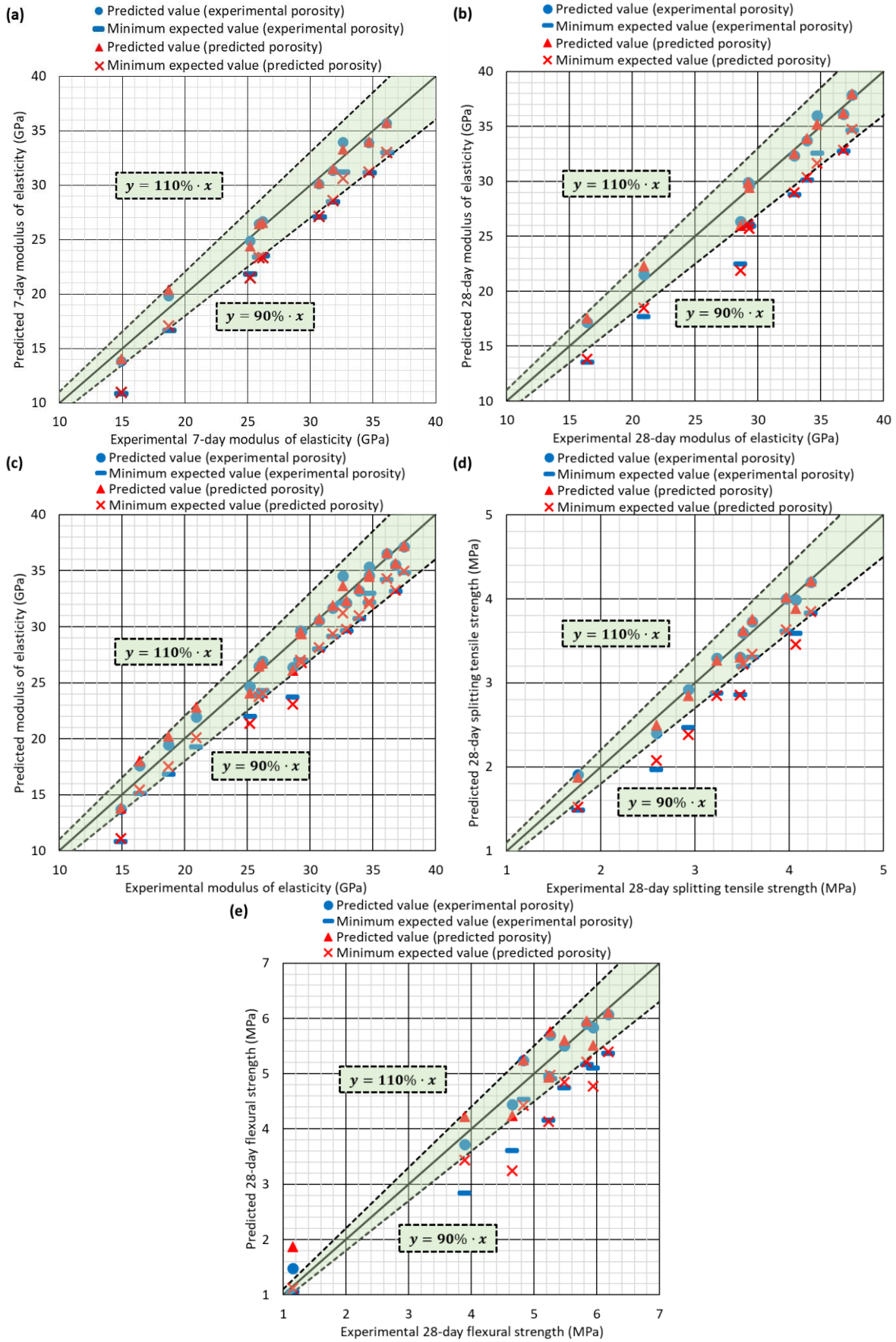
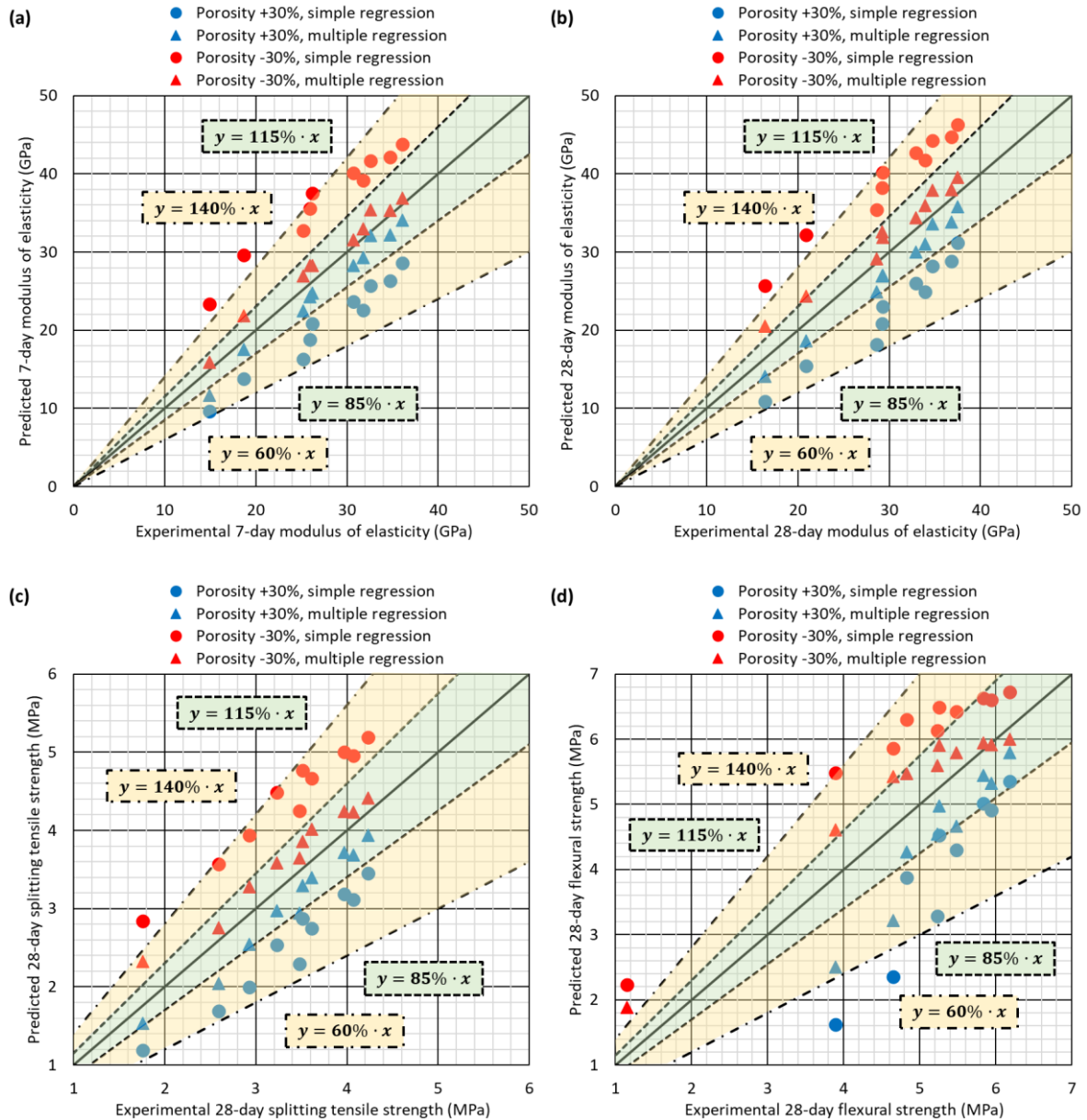


Figure 12. Comparison between experimental and predicted mechanical properties through multiple-regression models: (a) 7-day modulus of elasticity; (b) 28-day modulus of elasticity; (c) modulus of elasticity regardless of age; (d) 28-day splitting tensile strength; (e) 28-day flexural strength

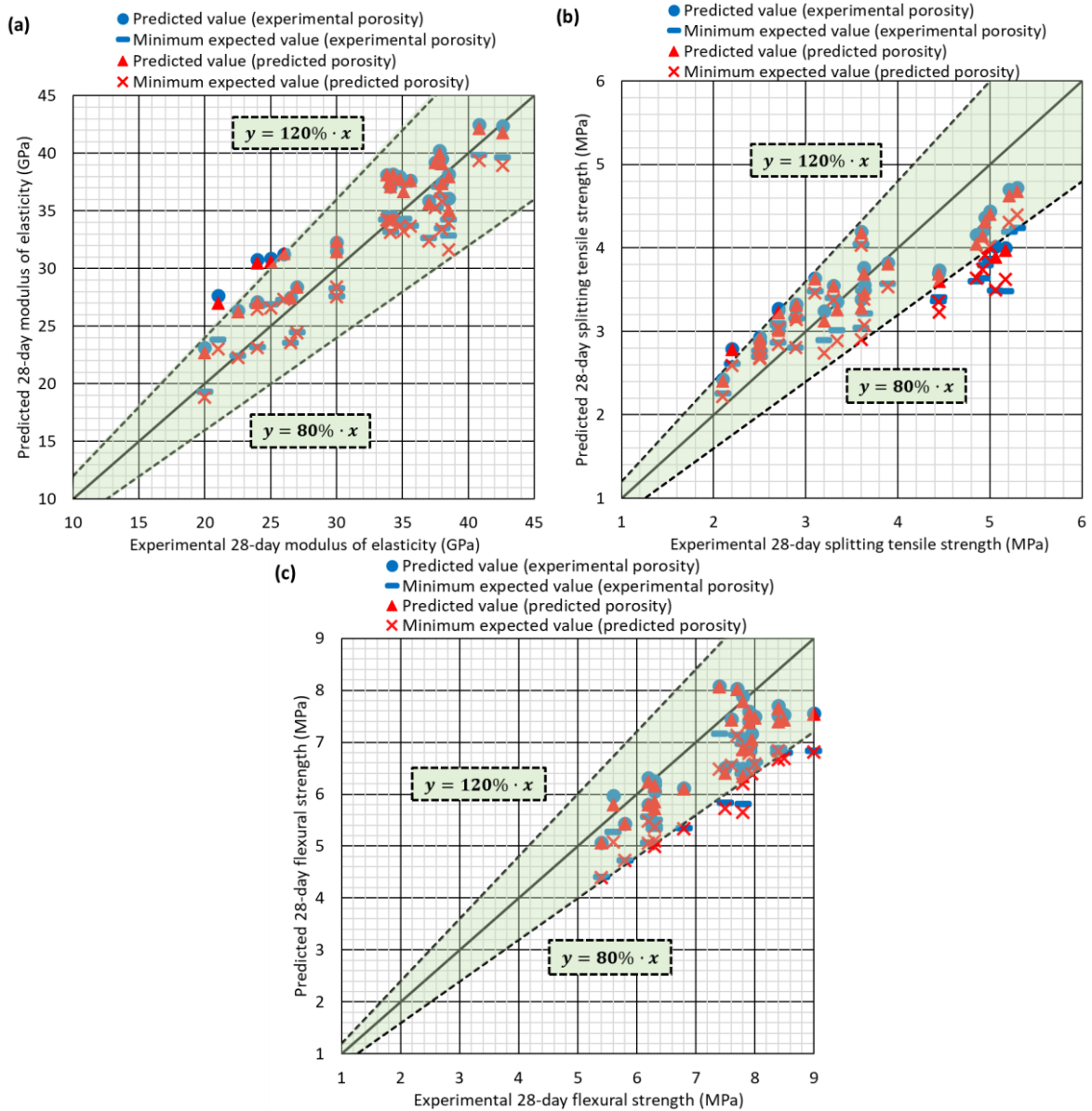


617
618
619
620
621
622
623
624
625
626
627
628
629
630
631
632
633
634
635
636
637
638
639
640
641
642
643
644
645
646
647
648
649
650
651
652
653
654
655
656
657
658
659
660
661
662
663
664
665

Figure 13. Effect of varying $\pm 30\%$ the experimental porosity on the estimation of the mechanical properties through simple-regression and multiple-regression models: (a) 7-day modulus of elasticity; (b) 28-day modulus of elasticity; (c) 28-day splitting tensile strength; (d) 28-day flexural strength

621 Underlining the greater robustness of prediction of the multiple-regression models regarding the porosity
622 value compared to simple-regression models, Figure 13 shows the comparison between the experimental
623 value and the value predicted by both types of models from an experimental porosity that was
624 underestimated or overestimated by 30%. The value estimated by the multiple-regression models only
625 deviated from the experimental value by 15% on average, a value very similar to the deviation obtained with
626 the correct porosity value, which was 10% (Figure 12). However, the values estimated by the simple-
627 regression models deviated from the experimental values by 40% on average, while this deviation was only
628 20% when using the correct value of porosity. Therefore, it is evident that an incorrect determination of
629 porosity has a lower impact on the predictive accuracy of multiple-regression models, due to the introduction
630 of compressive strength as a second predictive variable [37]. Both variables had a very similar influence on

631 the prediction of each mechanical property, hence the use of multiple-regression models statistically reduced
 632 by half the estimation errors caused by an incorrectly determined porosity.



633

634 Figure 14. Validation of multiple-regression models according to studies of the literature [16, 58, 67-71]: (a) 28-day modulus of
 635 elasticity; (b) 28-day splitting tensile strength; (c) 28-day flexural strength
 636

637 3.5.3. Validation of the models

638 Figure 13 can be considered a first validation of the models that were developed. This figure shows that the
 639 estimation of the mechanical properties through these models was correctly performed, even if there was a
 640 variation of the porosity, especially through the multiple-regression models. However, to guarantee the
 641 usefulness and reliability of the models, Figure 14 shows the comparison between the experimental value
 642 and the value estimated through the multiple-regression models of the 28-day mechanical properties
 643 collected in different studies of the literature [16, 58, 67-71]. All the concretes of these studies were SCC
 644 containing RCA, in line with the mixes of this research work, in which both mechanical properties and porosity

645 were determined. This validation was only performed with the multiple-regression models because they
646 were determined with the expressions from the simple regression models and because their use is
647 recommended, as indicated in the previous section.

648 As expected, the estimated mechanical properties of SCC from other studies were less accurate than that of
649 the concretes developed in this study from which the models were developed. However, at a 95% confidence
650 level, the estimated values only deviated by $\pm 20\%$ from the experimental ones. This limit is usually considered
651 adequate when predicting the mechanical properties of concrete, due to its high variability [72]. It can
652 therefore be affirmed that these models can yield adequate and safe values, regardless of whether the
653 experimentally measured porosity or the porosity estimated by Equation 5 is used for the prediction of the
654 mechanical properties. On the other hand, the minimum expected values were lower than the experimental
655 ones in most of the cases. The use of the minimum expected value was always adequate, ensuring the
656 reliability and safety of these values for structural design.

657 **4. Conclusions**

658 Throughout this study, the mechanical behavior (compressive strength, modulus of elasticity, splitting tensile
659 strength and flexural strength) and the effective porosity (capillary-water-absorption test) of a Self-
660 Compacting Concrete (SCC) made with 0%, 50% or 100% of coarse and/or fine Recycled Concrete Aggregate
661 (RCA) have been evaluated and likewise, the effect of the addition of RCA powder 0-1 mm. The following
662 conclusions can be drawn in relation to these properties and behavior:

- 663 • The addition of any RCA fraction worsened all mechanical properties. Fine RCA had a more
664 unfavorable effect than coarse RCA, although RCA powder was the most detrimental. No interaction
665 was detected between the effect of each RCA fraction on compressive strength, modulus of elasticity,
666 and flexural strength. There was only an interaction in splitting tensile strength, due to the increased
667 adhesion problems between the aggregate and the cementitious matrix when fine RCA was added
668 to the SCC that already contained coarse RCA. Therefore, in general, the decrease of strength and
669 elastic stiffness caused by the joint use of both RCA fractions was statistically equal to the sum of the
670 decreases caused by each fraction separately.
- 671 • RCA, especially the fine fraction, increased the effective porosity and water-absorption rate
672 (permeation coefficient and sorptivity) of SCC due to the appearance of larger pore sizes with higher
673 connectivity. Porosity could be estimated from the 24-h effective water (Equation 5), as this variable
674 reflected the higher porosity of SCC, due to the increase in water content when RCA was added, as
675 well as the affinity between the components of the mix from a statistical point of view.

676 The great novelty of this study are the models that have been developed, with which all the mechanical
677 properties of SCC with RCA may be predicted on the basis of concrete porosity. The use of this property

678 allows the expression to be the same regardless of the fraction of RCA added. Both simple-regression (Table
679 6) and multiple-regression models with compressive strength as secondary prediction variable (Table 7 and
680 Table 8) have been provided. The accuracy and reliability of these models has been validated through some
681 results of the literature. The conclusions that can be drawn regarding the use of these models are as follows:

- 682 • The accuracy of the simple-regression models ($\pm 20\%$ variation with respect to the experimental
683 value) was lower than that of the multiple-regression models ($\pm 10\%$ variation). Similarly, the
684 multiple-regression models showed greater robustness in the estimation of mechanical properties
685 when assuming a variation in porosity. This behavior was possible thanks to the introduction of
686 compressive strength as a secondary independent variable.
- 687 • The use of the estimated porosity (Equation 5) had no negative effects on the prediction of the
688 mechanical properties compared to the use of the experimental porosity. Therefore, the multiple-
689 regression models developed can be used by solely experimentally determining the compressive
690 strength, a commonly measured property in concrete in the industrial field. This allows a fast and
691 simple use of these models.
- 692 • The minimum expected values were lower than the experimental ones in most of the cases
693 regardless of the type of model and the porosity, experimental or predicted. Thus, their use when
694 performing any structural design will always be appropriate as they will never overestimate the
695 mechanical properties.

696 In view of the above, the authors consider that the models provided in this study are very useful for advancing
697 the use of RCA concrete. The authors recommend the use of the multiple-regression models, due to their
698 higher accuracy and robustness. However, the models developed are only valid for SCC, so research still has
699 immense breadth in this field and models could be developed for other types of concrete, such as vibrated
700 concrete, and high-performance concrete.

701 **Acknowledgements**

702 The authors wish to express their gratitude to: Spanish Ministry of Universities within the framework of the
703 State Program for the Promotion of Talent and its Employability in R+D+i, State Mobility Subprogram, of the
704 State Plan for Scientific and Technical Research and Innovation 2017-2020 [PRX21/00007]; the Spanish
705 Ministry MCI, AEI, EU and ERDF [grant numbers PID2020-113837RB-I00; 10.13039/501100011033;
706 FPU17/03374]; the Junta de Castilla y León (Regional Government) and ERDF [grant numbers UIC-231;
707 BU119P17]; Youth Employment Initiative (JCyL) and ESF [grant number UBU05B_1274]; and finally, the
708 University of Burgos [grant numbers SUCONS, Y135.GI] and the University of Padova.

709 **Conflict of interest**

710 The authors declare that there is no conflict of interest.

711 **References**

- 712 [1] V. Ortega-López, J.A. Fuente-Alonso, A. Santamaría, J.T. San-José, Á. Aragón, Durability studies on fiber-
713 reinforced EAF slag concrete for pavements, *Constr. Build. Mater.* 163 (2018) 471-481.
714 <https://doi.org/10.1016/j.conbuildmat.2017.12.121>.
- 715 [2] W. Soja, F. Georget, H. Maraghechi, K. Scrivener, Evolution of microstructural changes in cement paste
716 during environmental drying, *Cem. Concr. Res.* 134 (2020) 106093.
717 <https://doi.org/10.1016/j.cemconres.2020.106093>.
- 718 [3] L. Zingg, M. Briffaut, J. Baroth, Y. Malecot, Influence of cement matrix porosity on the triaxial behaviour
719 of concrete, *Cem. Concr. Res.* 80 (2016) 52-59. <https://doi.org/10.1016/j.cemconres.2015.10.005>.
- 720 [4] A. du Plessis, W.P. Boshoff, A review of X-ray computed tomography of concrete and asphalt construction
721 materials, *Constr. Build. Mater.* 199 (2019) 637-651. <https://doi.org/10.1016/j.conbuildmat.2018.12.049>.
- 722 [5] A. Koenig, Analysis of air voids in cementitious materials using micro X-ray computed tomography (μ XCT),
723 *Constr. Build. Mater.* 244 (2020) 118313. <https://doi.org/10.1016/j.conbuildmat.2020.118313>.
- 724 [6] P. Basu, B.S. Thomas, R. Chandra Gupta, V. Agrawal, Strength, permeation, freeze-thaw resistance, and
725 microstructural properties of self-compacting concrete containing sandstone waste, *J. Clean. Prod.* 305
726 (2021) 127090. <https://doi.org/10.1016/j.jclepro.2021.127090>.
- 727 [7] M. Thiam, M. Fall, Engineering properties of a building material with melted plastic waste as the only
728 binder, *J. Build. Eng.* 44 (2021) 102684. <https://doi.org/10.1016/j.jobbe.2021.102684>.
- 729 [8] J. Nobre, M. Bravo, J. de Brito, G. Duarte, Durability performance of dry-mix shotcrete produced with
730 coarse recycled concrete aggregates, *J. Buil. Eng.* 29 (2020) 101135.
731 <https://doi.org/10.1016/j.jobbe.2019.101135>.
- 732 [9] B. Cantero, M. Bravo, J. de Brito, I.F. Sáez del Bosque, C. Medina, Water transport and shrinkage in
733 concrete made with ground recycled concrete-additioned cement and mixed recycled aggregate, *Cem. Concr.*
734 *Compos.* 118 (2021) 103957. <https://doi.org/10.1016/j.cemconcomp.2021.103957>.
- 735 [10] A. Santamaría, A. Orbe, J.T. San José, J.J. González, A study on the durability of structural concrete
736 incorporating electric steelmaking slags, *Constr. Build. Mater.* 161 (2018) 94-111.
737 <https://doi.org/10.1016/j.conbuildmat.2017.11.121>.
- 738 [11] G. Chen, F. Li, J. Geng, P. Jing, Z. Si, Identification, generation of autoclaved aerated concrete pore
739 structure and simulation of its influence on thermal conductivity, *Constr. Build. Mater.* 294 (2021) 123572.
740 <https://doi.org/10.1016/j.conbuildmat.2021.123572>.
- 741 [12] J. Mínguez, M.A. Vicente, D.C. González, Pore morphology variation under ambient curing of plain and
742 fiber-reinforced high performance mortar at an early age, *Constr. Build. Mater.* 198 (2019) 718-731.
743 <https://doi.org/10.1016/j.conbuildmat.2018.12.010>.

744 [13] R. Wang, N. Yu, Y. Li, Methods for improving the microstructure of recycled concrete aggregate: A review,
1 745 *Constr. Build. Mater.* 242 (2020) 118164. <https://doi.org/10.1016/j.conbuildmat.2020.118164>.
2
3 746 [14] K.C. Hover, The influence of water on the performance of concrete, *Constr. Build. Mater.* 25 (7) (2011)
4 747 3003-3013. <https://doi.org/10.1016/j.conbuildmat.2011.01.010>.
5
6 748 [15] M.A. Vicente, J. Mínguez, D.C. González, Computed tomography scanning of the internal microstructure,
7 749 crack mechanisms, and structural behavior of fiber-reinforced concrete under static and cyclic bending tests,
8 750 *Int. J. Fatigue* 121 (2019) 9-19. <https://doi.org/10.1016/j.ijfatigue.2018.11.023>.
9
10 751 [16] F. Fiol, C. Thomas, J.M. Manso, I. López, Transport mechanisms as indicators of the durability of precast
11 752 recycled concrete, *Constr. Build. Mater.* 269 (2021) 121263.
12 753 <https://doi.org/10.1016/j.conbuildmat.2020.121263>.
13
14 754 [17] I. Pundienė, J. Pranckevičienė, M. Kligys, O. Kizinievič, The synergetic interaction of chemical admixtures
15 755 on the properties of eco-friendly lightweight concrete from industrial technogenic waste, *Constr. Build.*
16 756 *Mater.* 256 (2020) 119461. <https://doi.org/10.1016/j.conbuildmat.2020.119461>.
17
18 757 [18] J.T. San-José, J.M. Manso, Fiber-reinforced polymer bars embedded in a resin concrete: Study of both
19 758 materials and their bond behavior, *Polym. Compos.* 27 (3) (2006) 315-322.
20 759 <https://doi.org/10.1002/pc.20188>.
21
22 760 [19] S. Zhu, C. Wu, H. Yin, Virtual experiments of particle mixing process with the sph-dem model, *Materials*
23 761 14 (9) (2021) 2199. <https://doi.org/10.3390/ma14092199>.
24
25 762 [20] T. Sugamata, M. Hibino, M. Ouchi, H. Okamura, Study of the particle dispersion effect of polycarboxylate-
26 763 based superplasticizers, *Trans. Jpn. Concr. Inst.* 21 (1999) 7-14.
27
28 764 [21] M. Ouchi, Y. Edamatsu, K. Ozawa, H. Okamura, Simple evaluation method for interaction between coarse
29 765 aggregate and mortar's particles in self-compacting concrete, *Trans. Jpn. Concr. Inst.* 21 (1999) 1-6.
30
31 766 [22] A. Santamaría, A. Orbe, M.M. Losañez, M. Skaf, V. Ortega-Lopez, J.J. González, Self-compacting concrete
32 767 incorporating electric arc-furnace steelmaking slag as aggregate, *Mater. Des.* 115 (2017) 179-193.
33 768 <https://doi.org/10.1016/j.matdes.2016.11.048>.
34
35 769 [23] M.O. Valcuende, C. Parra, J. Benlloch, Permeability, porosity and compressive strength of self-
36 770 compacting concretes, *Mater. Constr.* 55 (280) (2005) 17-26. <https://doi.org/10.3989/mc.2005.v55.i280.203>.
37
38 771 [24] E.R. Teixeira, A. Camões, F.G. Branco, J.C. Matos, Effect of biomass fly ash on fresh and hardened
39 772 properties of high volume fly ash mortars, *Crystals* 11 (3) (2021) 233. <https://doi.org/10.3390/cryst11030233>.
40
41 773 [25] I.O.R. Areias, C.M.F. Vieira, H.A. Colorado, G.C.G. Delaqua, S.N. Monteiro, A.R.G. Azevedo, Could city
42 774 sewage sludge be directly used into clay bricks for building construction? A comprehensive case study from
43 775 Brazil, *J. Build. Eng.* 31 (2020) 101374. <https://doi.org/10.1016/j.jobe.2020.101374>.
44
45 776 [26] G.C. Girondi Delaqua, M.T. Marvila, D. Souza, R.J. Sanchez Rodriguez, H.A. Colorado, C.M. Fontes Vieira,
46 777 Evaluation of the application of macrophyte biomass *Salvinia auriculata* Aublet in red ceramics, *J. Environ.*
47 778 *Manage.* 275 (2020) 111253. <https://doi.org/10.1016/j.jenvman.2020.111253>.
48
49
50
51
52
53
54
55
56
57
58
59
60
61
62
63
64
65

779 [27] V. Revilla-Cuesta, M. Skaf, F. Faleschini, J.M. Manso, V. Ortega-López, Self-compacting concrete
1 780 manufactured with recycled concrete aggregate: An overview, *J. Clean. Prod.* 262 (2020) 121362.
2 781 <https://doi.org/10.1016/j.jclepro.2020.121362>.
3 782 [28] A.R. Khan, S. Fareed, M.S. Khan, Use of recycled concrete aggregates in structural concrete, *Sustain.*
4 783 *Constr. Mater. Technol.* 2 (2019).
5 784 [29] R.V. Silva, J. De Brito, R.K. Dhir, Establishing a relationship between modulus of elasticity and
6 785 compressive strength of recycled aggregate concrete, *J. Clean. Prod.* 112 (2016) 2171-2186.
7 786 <https://doi.org/10.1016/j.jclepro.2015.10.064>.
8 787 [30] R.V. Silva, J. De Brito, R.K. Dhir, The influence of the use of recycled aggregates on the compressive
9 788 strength of concrete: A review, *Eur. J. Environ. Civ. Eng.* 19 (7) (2015) 825-849.
10 789 <https://doi.org/10.1080/19648189.2014.974831>.
11 790 [31] V.W.Y. Tam, K. Wang, C.M. Tam, Assessing relationships among properties of demolished concrete,
12 791 recycled aggregate and recycled aggregate concrete using regression analysis, *J. Hazard. Mater.* 152 (2)
13 792 (2008) 703-714. <https://doi.org/10.1016/j.jhazmat.2007.07.061>.
14 793 [32] V. Revilla-Cuesta, V. Ortega-López, M. Skaf, J.M. Manso, Effect of fine recycled concrete aggregate on
15 794 the mechanical behavior of self-compacting concrete, *Constr. Build. Mater.* 263 (2020) 120671.
16 795 <https://doi.org/10.1016/j.conbuildmat.2020.120671>.
17 796 [33] J. Huang, C. Zou, D. Sun, B. Yang, J. Yan, Effect of recycled fine aggregates on alkali-activated slag concrete
18 797 properties, *Structures* 30 (2021) 89-99. <https://doi.org/10.1016/j.istruc.2020.12.064>.
19 798 [34] S.K. Kirthika, S.K. Singh, Durability studies on recycled fine aggregate concrete, *Constr. Build. Mater.* 250
20 799 (2020) 118850. <https://doi.org/10.1016/j.conbuildmat.2020.118850>.
21 800 [35] F. Fiol, C. Thomas, C. Muñoz, V. Ortega-López, J.M. Manso, The influence of recycled aggregates from
22 801 precast elements on the mechanical properties of structural self-compacting concrete, *Constr. Build. Mater.*
23 802 182 (2018) 309-323. <https://doi.org/10.1016/j.conbuildmat.2018.06.132>.
24 803 [36] D. Carro-López, B. González-Fonteboa, J. De Brito, F. Martínez-Abella, I. González-Taboada, P. Silva, Study
25 804 of the rheology of self-compacting concrete with fine recycled concrete aggregates, *Constr. Build. Mater.* 96
26 805 (2015) 491-501. <https://doi.org/10.1016/j.conbuildmat.2015.08.091>.
27 806 [37] V. Revilla-Cuesta, M. Skaf, A.B. Espinosa, A. Santamaría, V. Ortega-López, Statistical approach for the
28 807 design of structural self-compacting concrete with fine recycled concrete aggregate, *Mathematics* 8 (12)
29 808 (2020) 2190. <https://doi.org/10.3390/math8122190>.
30 809 [38] EN-Euronorm, Rue de stassart, 36. Belgium-1050 Brussels, European Committee for Standardization.
31 810 [39] F. Agrela, M. Sánchez De Juan, J. Ayuso, V.L. Geraldes, J.R. Jiménez, Limiting properties in the
32 811 characterisation of mixed recycled aggregates for use in the manufacture of concrete, *Constr. Build. Mater.*
33 812 25 (10) (2011) 3950-3955. <https://doi.org/10.1016/j.conbuildmat.2011.04.027>.

813 [40] A. Santamaría, J.J. González, M.M. Losáñez, M. Skaf, V. Ortega-López, The design of self-compacting
1 814 structural mortar containing steelmaking slags as aggregate, *Cem. Concr. Compos.* 111 (2020) 103627.
2 815 <https://doi.org/10.1016/j.cemconcomp.2020.103627>.
3 816 [41] EC2, Eurocode 2: Design of concrete structures. Part 1-1: General rules and rules for buildings, CEN
4 817 (European Committee for Standardization) (2010).
5 818 [42] S. Santos, P.R. da Silva, J. de Brito, Self-compacting concrete with recycled aggregates – A literature
6 819 review, *J. Build. Eng.* 22 (2019) 349-371. <https://doi.org/10.1016/j.job.2019.01.001>.
7 820 [43] M. Bravo, J. De Brito, J. Pontes, L. Evangelista, Mechanical performance of concrete made with
8 821 aggregates from construction and demolition waste recycling plants, *J. Clean. Prod.* 99 (2015) 59-74.
9 822 <https://doi.org/10.1016/j.jclepro.2015.03.012>.
10 823 [44] E. Güneysi, M. Gesoğlu, Z. Algin, H. Yazici, Effect of surface treatment methods on the properties of self-
11 824 compacting concrete with recycled aggregates, *Constr. Build. Mater.* 64 (2014) 172-183.
12 825 <https://doi.org/10.1016/j.conbuildmat.2014.04.090>.
13 826 [45] RILEM, CPC 11.2, Absorption of Water by Concrete by Capillarity (1982).
14 827 [46] F. Faleschini, C. Jiménez, M. Barra, D. Aponte, E. Vázquez, C. Pellegrino, Rheology of fresh concretes with
15 828 recycled aggregates, *Constr. Build. Mater.* 73 (2014) 407-416.
16 829 <https://doi.org/10.1016/j.conbuildmat.2014.09.068>.
17 830 [47] V. Revilla-Cuesta, M. Skaf, A. Santamaría, J.J. Hernández-Bagaces, V. Ortega-López, Temporal flowability
18 831 evolution of slag-based self-compacting concrete with recycled concrete aggregate, *J. Clean. Prod.* 299 (2021)
19 832 126890. <https://doi.org/10.1016/j.jclepro.2021.126890>.
20 833 [48] Á. Salesa, J.Á. Pérez-Benedicto, L.M. Esteban, R. Vicente-Vas, M. Orna-Carmona, Physico-mechanical
21 834 properties of multi-recycled self-compacting concrete prepared with precast concrete rejects, *Constr. Build.*
22 835 *Mater.* 153 (2017) 364-373. <https://doi.org/10.1016/j.conbuildmat.2017.07.087>.
23 836 [49] M. Nedeljković, J. Visser, B. Šavija, S. Valcke, E. Schlangen, Use of fine recycled concrete aggregates in
24 837 concrete: A critical review, *J. Build. Eng.* 38 (2021) 102196. <https://doi.org/10.1016/j.job.2021.102196>.
25 838 [50] M. Gesoglu, E. Güneysi, H.Ö. Öz, I. Taha, M.T. Yasemin, Failure characteristics of self-compacting
26 839 concretes made with recycled aggregates, *Constr. Build. Mater.* 98 (2015) 334-344.
27 840 <https://doi.org/10.1016/j.conbuildmat.2015.08.036>.
28 841 [51] S.A. Santos, P.R. da Silva, J. de Brito, Mechanical performance evaluation of self-compacting concrete
29 842 with fine and coarse recycled aggregates from the precast industry, *Materials* 10 (8) (2017) 904.
30 843 <https://doi.org/10.3390/ma10080904>.
31 844 [52] B. Cantero, I.F. Sáez del Bosque, A. Matías, M.I. Sánchez de Rojas, C. Medina, Inclusion of construction
32 845 and demolition waste as a coarse aggregate and a cement addition in structural concrete design, *Arch. Civ.*
33 846 *Mech. Eng.* 19 (4) (2019) 1338-1352. <https://doi.org/10.1016/j.acme.2019.08.004>.

847 [53] S.T. Yildirim, C. Meyer, S. Herfellner, Effects of internal curing on the strength, drying shrinkage and
1 848 freeze-thaw resistance of concrete containing recycled concrete aggregates, *Constr. Build. Mater.* 91 (2015)
2 849 288-296. <https://doi.org/10.1016/j.conbuildmat.2015.05.045>.
3
4 850 [54] A. Gonzalez-Corominas, M. Etxeberria, Effects of using recycled concrete aggregates on the shrinkage of
5 851 high performance concrete, *Constr. Build. Mater.* 115 (2016) 32-41.
6 852 <https://doi.org/10.1016/j.conbuildmat.2016.04.031>.
7
8 853 [55] S. Boudali, B. Abdulsalam, A.H. Rafiean, S. Poncet, A. Soliman, A. Elsafty, Influence of fine recycled
9 854 concrete powder on the compressive strength of self-compacting concrete (Scc) using artificial neural
10 855 network, *Sustainability* 13 (6) (2021) 3111. <https://doi.org/10.3390/su13063111>.
11
12 856 [56] W.C. Tang, P.C. Ryan, H.Z. Cui, W. Liao, Properties of Self-Compacting Concrete with Recycled Coarse
13 857 Aggregate, *Adv. Mater. Sci. Eng.* 2016 (2016) 2761294. <https://doi.org/10.1155/2016/2761294>.
14
15 858 [57] S.C. Kou, C.S. Poon, Properties of self-compacting concrete prepared with coarse and fine recycled
16 859 concrete aggregates, *Cem. Concr. Compos.* 31 (9) (2009) 622-627.
17 860 <https://doi.org/10.1016/j.cemconcomp.2009.06.005>.
18
19 861 [58] Z. Duan, A. Singh, J. Xiao, S. Hou, Combined use of recycled powder and recycled coarse aggregate
20 862 derived from construction and demolition waste in self-compacting concrete, *Constr. Build. Mater.* 254
21 863 (2020) 119323. <https://doi.org/10.1016/j.conbuildmat.2020.119323>.
22
23 864 [59] UNE 83966, Concrete durability. Test methods. Conditioning of concrete test pieces for the purpose of
24 865 gas permeability and capilar suction tests (2008).
25
26 866 [60] R.V. Silva, J. de Brito, R.K. Dhir, Fresh-state performance of recycled aggregate concrete: A review,
27 867 *Constr. Build. Mater.* 178 (2018) 19-31. <https://doi.org/10.1016/j.conbuildmat.2018.05.149>.
28
29 868 [61] G. Puente de Andrade, G. de Castro Polisseni, M. Pepe, R.D. Toledo Filho, Design of structural concrete
30 869 mixtures containing fine recycled concrete aggregate using packing model, *Constr. Build. Mater.* 252 (2020)
31 870 119091. <https://doi.org/10.1016/j.conbuildmat.2020.119091>.
32
33 871 [62] UNE 83982, Concrete durability. Test methods. Determination of the capillar suction in hardened
34 872 concrete. Fagerlund method (2008).
35
36 873 [63] B. Cantero, I.F. Sáez del Bosque, A. Matías, M.I. Sánchez de Rojas, C. Medina, Water transport
37 874 mechanisms in concretes bearing mixed recycled aggregates, *Cem. Concr. Compos.* 107 (2020) 103486.
38 875 <https://doi.org/10.1016/j.cemconcomp.2019.103486>.
39
40 876 [64] P. Anaya, J. Rodríguez, C. Andrade, B. Martín-Pérez, C.L. Hombrados, Determination of wires transfer
41 877 length in prestressed concrete members with different levels of corrosion, *Inf. Constr.* 72 (558) (2020) 1-10.
42 878 <https://doi.org/10.3989/ic.71428>.
43
44 879 [65] Y. Yu, Y. Zheng, J.J. Xu, X.L. Wang, Modeling and predicting the mechanical behavior of concrete under
45 880 uniaxial loading, *Constr. Build. Mater.* 273 (2021) 121694.
46 881 <https://doi.org/10.1016/j.conbuildmat.2020.121694>.
47
48
49
50
51
52
53
54
55
56
57
58
59
60
61
62
63
64
65

882 [66] ACI-318-19, Building Code Requeriments for Structural Concrete (2019).

1
2 883 [67] M. Abed, R. Nemes, B.A. Tayeh, Properties of self-compacting high-strength concrete containing multiple
3 884 use of recycled aggregate, J. King Saud Univ. Eng. Sci. 32 (2) (2020) 108-114.
4
5 885 <https://doi.org/10.1016/j.jksues.2018.12.002>.

6
7 886 [68] M. Omrane, M. Rabehi, Effect of natural pozzolan and recycled concrete aggregates on thermal and
8
9 887 physico-mechanical characteristics of self-compacting concrete, Constr. Build. Mater. 247 (2020) 118576.
10 888 <https://doi.org/10.1016/j.conbuildmat.2020.118576>.

11
12 889 [69] P. Rajhans, S.K. Panda, S. Nayak, Sustainability on durability of self compacting concrete from C&D waste
13
14 890 by improving porosity and hydrated compounds: A microstructural investigation, Constr. Build. Mater. 174
15
16 891 (2018) 559-575. <https://doi.org/10.1016/j.conbuildmat.2018.04.137>.

17
18 892 [70] A. Sadeghi-Nik, J. Berenjian, S. Alimohammadi, O. Lotfi-Omran, A. Sadeghi-Nik, M. Karimaei, The Effect
19
20 893 of Recycled Concrete Aggregates and Metakaolin on the Mechanical Properties of Self-Compacting Concrete
21 894 Containing Nanoparticles, Iran. J. Sci. Tech. Trans. Civ. Eng. 43 (2019) 503-515.
22
23 895 <https://doi.org/10.1007/s40996-018-0182-4>.

24
25 896 [71] K. Zitouni, A. Djerbi, A. Mebrouki, Study on the microstructure of the new paste of recycled aggregate
26
27 897 self-compacting concrete, Materials 13 (9) (2020) 2114. <https://doi.org/10.3390/ma13092114>.

28 898 [72] J.C. Salcedo, M. Fortea, The influence of structural alterations on the damages of the Amatrice
29
30 899 earthquake, Italy (2016), Inf. Constr. 72 (559) (2020) 71378. <https://doi.org/10.3989/IC.71378>.

Declaration of interests

The authors declare that they have no known competing financial interests or personal relationships that could have appeared to influence the work reported in this paper.

The authors declare the following financial interests/personal relationships which may be considered as potential competing interests: